On berm breakwaters

- an investigation into recession and overtopping -

Adrian Bãtãcui Radu Ciocan

Aalborg University M.Sc in Structural and Civil Engineering Master Thesis, Spring 2013

School of Engineering and Science
Aalborg University
Sohngaardsholmsvej 57
9000 Aalborg

Title:
On berm breakwaters
- an investigaion into recession and overtopping -

Project period:
Master, spring 2013

Project group:
B107

Authors:

_____
Adrian Bătăcui

_____
Radu Catalin Ciocan

Supervisor:

_____
Thomas Lykke Andersen

Copies: 6
Pages: 82
Number of appendices: 5
Pages in appendix: 21
Completed: 13-06-2013

Synopsis:

The front slope stability and berm recession of berm breakwaters has been the subject of several important studies, and many important findings have been made in recent years. At the moment, there are several ways of calculating berm recession. Much of the progress made in the field of berm breakwaters has been based on the work by Jentsje van der Meer, and, more recently, Thomas Lykke-Andersen.
In this Master Thesis, some of the more promising berm recession estimation formulas are evaluated. An experimental procedure is planned and a total of 55 tests are performed. The main parameters varied in these tests are the stability numbers, front slope, and berm height. Several sea states are also tested.
The investigation highlites several parameters used in the formulas and their importance. A change to the Lykke-Andersen formula is porposed, which leads to a better fit with the current data. Also, the formation of a step is studied with the use of a MatLab code specially made for this purpose.
Relatively new formulas, such as Moghim and Shekari, are also tested against the current data, and some suggestions are made for future investigations.

Preface

The work for this Master Thesis, entitled *On berm breakwaters - an investigaion into recession and overtopping*, and the writing of the thesis itself has been carried out between the 1st of February 2013 and the 13th of June 2013 at the Department of Civil Engineering of Aalborg University, Denmark, under the supervision of Professor Thomas Lykke-Andersen.

The thesis is divided into three parts. The first part consists of an introduction, followed by a problem analysis, where the subject of the report is investigated and a goal for the research is formulated. The second part detailes the design of experimental procedures, followed by an overview of model testing and results. The third and last part consists of an analysis of test data for the purpose stated in the problem analysis. The findings of this report are summarised in a conclusion at the end of the paper.

The thesis comprises of chapters, sections, and subsections, which are numbered sequentially in the order of appearance. The chapters are grouped into parts, which are numbered using roman numerals. The Appendix is organized into chapters, which are not numbered but alphabetized, e.g., *A* is the first appendix, *B* is the second, etc. An appendix DVD is also attached to the report, containing the collected data from the experiments, as well as the codes created by the group.

Tables and figures are numbered according to the chapter in which they appear. Captions are located below each figure, and above each table. When a chapter, section, subsection, figure, table, or equation is referenced in the text, the reference will apear with a capital first letter, e.g., *Figure 1.1*, *Chapter 1*, etc.

Within the report, different studies and other sources are referenced. A list of referenced sources is available at the end of the main report. The Harvard method is used to make references. In the text, references appear as the name of the authors, followed by the year. If a source more than two authors, the names of all authors only appear in the first reference to the respective source in each chapter. In subsequent references, the abbreviation et al. will be used for all but the main author, e.g. *Tørum et al. [2011]*.

Acknowledgements
The group behind this project would like to express their appreciation to the people that greatly assisted in the work leading to this report, and the writing of the paper itself. We would like to acknowledge the valuable advice and guidance of Professor Thomas Lykke-Andersen, the project supervisor. Also, we would like to thank the laboratory staff at the Department of Civil Engineering for their assistance in setting up and conducting model tests. Special thanks should be given to Palle Meinert, who offered his time and knowledge to our aid in understanding the instrumentation of our experiments. Finally, we would like to express our gratitude to our loved ones, who always provided emotional and finantial assistance.

The authors,
Adrian Bătăcui
RaduCiocan

Aalborg, 13.06.2013

Contents

List of symbols

Symbol	Name	Unit
α_d	angle of front slope	$[^\circ]$
δ	relative reduced mass density	$[-]$
ν	kinematic viscosity (water)	$[m^2/s]$
ρ_s	mass density of stones	$[kg/m^3]$
ρ_w	mass density of water	$[kg/m^3]$
ξ	surf similarity parameter	$[-]$
A_e	eroded area	$[m^2]$
$B_\star$	dimentionless berm width	$[-]$
b_1	skewness	$[-]$
d	water depth in front of the structure	$[m]$
$D_{n,50}$	median equivalent cubic length	$[m]$
f_β	incident wave angle factor	$[-]$
f_{grad}	stone gradation factor	$[-]$
f_{h0}	stability index factor	$[-]$
f_{hb}	berm elevation factor	$[-]$
f_{sk}	skewness factor	$[-]$
f_d	depth factor	$[-]$
f_g	gradation factor	$[-]$
f_N	number of waves factor	$[-]$
g	gravitational acceleration	$[m/s^2]$ *or* $[N/kg]$
$G_\star$	dimensionless armor crest width	$[-]$
h	water depth in front of the structure	$[m]$
$h_{b\star}$	dimensionless berm elevation	$[-]$
h_{br}	berm elevation	$[m]$
H_{m0}	significant wave height, frequency domain	$[m]$
H_0	stability number	$[-]$
H_0T_0	stability number including wave period	$[-]$
h_b	water depth above berm	$[m]$
h_f	depth of profile intersection point	$[m]$
h_s	step height	$[m]$
H_s	significant wave height, time domain	$[m]$
k_p	peak wave number	$[-]$
L_{0m}	mean deep water wave length	$[m]$
L_p	peak wave length	$[m]$
N	number of waves	$[-]$

P	permeability	$[-]$
q	average overtopping discharge rate	$[m^3/m/s]$
$Q_\star$	dimentionless mean overtopping discharge	$[-]$
$R_\star$	dimensionless crest freeboard	$[-]$
R_c	crest freeboard	$[m]$
Re	Reynolds number	$[-]$
Rec	berm recession	$[m]$
S	damage	$[-]$
s_{0m}	mean wave steepness	$[-]$
SWL	still water level	$[m]$
$T_{0,1}$	spectral mean wave period	$[s]$
T_0	stability number based on wave period	$[-]$
T_0^*	dimentionless wave period transition point	$[-]$
Ur	Ursell number	$[-]$
W_{50}	median mass of stones	$[kg]$

Part I

Introduction

1 Introduction

Breakwaters have always had an important role in sheltering the harbor basin from the violent forces of the surrounding sea. One of the rather new structures used for this purposes is the berm breakwater.

Berm breakwaters were introduced in the early 1980's as an alternative to traditional rubble mound breakwaters. Their main advantage is that smaller stones can be used for the front armor layer without compromising stability. This is due to the fact that the stones which make up the front armor layer are allowed to move in order to have it designed by the wave climate into a much more stable profile.

Using this principle, the construction of a berm breakwater does not require special equipment necessary for lifting heavy armor stones; instead conventional contractors equipment can be used, thus reducing the construction costs.

In terms of stability, there are two main categories of berm breakwaters:

1. Statically Stable:

- Non-reshaped Statical Stable: only some few stones are allowed to move; similar to what is allowed on a conventional rubble mound breakwater
- Reshaped Statical Stable: the profile is reshaped into a stable profile where the individual stones are also stable.

2. Dynamically Stable: the profile is reshaped into a stable profile, but the individual stones may still move up and down the slope.

The study will consist on investigating the stability of the seaward part of the berm breakwater regarding the displacement of the armor layer material. An example of a comparison between a initial and a reshaped (damaged) profile is illustrated in Figure 1.1, it can be seen that the amount of damage a breakwater has sustained can be described by the Recession parameter, Rec and eroded area, A_e.

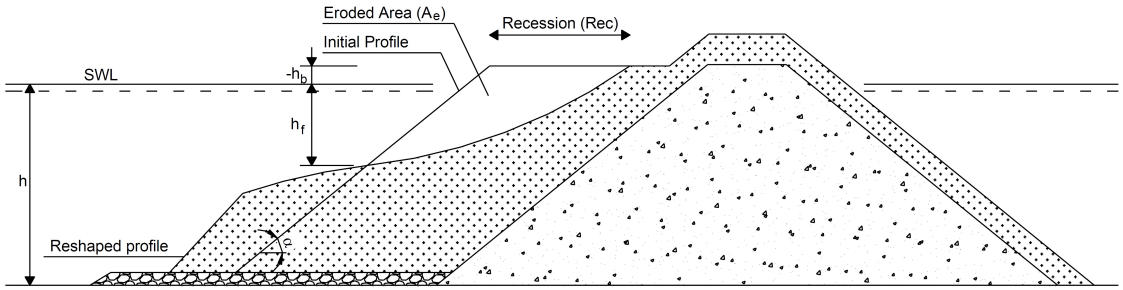

Figure 1.1. Initial vs. Reshaped berm breakwater profile. [Lykke Andersen et al. (2012)]

It is expected that by modifying certain structural parameters, e.g. the front armor layer angle, height of the berm, one can reduce the amount of damage (Recession), the breakwater will be subjected to.

Van der Meer (1988) and T. Lykke Andersen et al. (2012) are taken as guidelines for this project. Thus, in order to add more to the present knowledge, this project will

focus on investigating different berm recession formulas, the variables they take into account and the influence those variables have. An analysis will be made on the use of those parameters and, where needed, some changes may be proposed. As a secondary objective, the stability of berm breakwaters will be studied in relation to Van der Meer (1988). In addition a short analysis of the overtopping will be made using one of the most promissing overtopping estimation method.

2 Problem analysis

Berm breakwaters are traditionally designed to reshape, making the berm recession one of the most important parameters to investigate when dealing with such breakwaters. There are many different projects that had the goal of delivering a formula capable of estimating the recession. Different projects choose different sea states for their laboratory tests and so the resulted formulas will, in most cases, apply only for those sea states.

In this section, the most promising methods will be described and also, their limits will be illustrated. These limits will then be the reference points for this project's laboratory investigations with the goal of determining which limits can be extended for each of the presented methods.

The following methods for estimating berm recession will be discussed :

- van der Meer [1988]
- Tørum and Krogh [2000]
- Lykke Andersen and Burcharth [2009]
- Moghim, Shafieefar, Tørum, and Chegini [2011]
- Shekari and Shafieefar [2012]

2.1 Armour layer stability

Determining armour layer stability is a matter of balancing the stabilizing factors (weight of the individual armor rocks), and de-stabilizing factors, such as drag and lift (explained in Appendix 1). Currently, the most used stability parameters are the ones introduced by Hudson and van der Meer. They are detailed in the following.

The first parameter that describes the stability of the breakwater is H_0. This parameter is defined in Equation (2.1). In Equation (2.2), K_D is a dimensionless parameter that depends on the type of armour used. Lykke Andersen [2006] advises caution in the selection of K_D, as it is difficult to assign a definite value. As a rule of thumb, values of 1.0 to 4.0 are recommended for rock armour.

$$H_0 = \frac{H_{m0}}{\Delta \cdot D_{n,50}} \tag{2.1}$$

$$H_0 = (K_D \cdot cot(\alpha))^{1/3} \tag{2.2}$$

The equivalent cube length, $D_{n,50}$, is defined by Equation (2.3).

$$D_{n,50} = \left(\frac{W_{50}}{\rho_s}\right)^{1/3} \tag{2.3}$$

$$\Delta = \frac{\rho_s}{\rho_w} - 1 \tag{2.4}$$

Where:

H_{m0}	wave height	$[m]$
Δ	relative reduced mass density	$[-]$
ρ_s	mass density of stones	$[kg/m^3]$
ρ_w	mass density of water	$[kg/m^3]$
$W_{n,50}$	median weight of stones	$[kg]$

For the stability number defined in Equation (2.1), van der Meer proposes an empirical formula, depending on breaker type. The formula is presented in Equation (2.5). These equations have been developed for straight, non-overtopped slopes. An important parameter also introduced for this equation is the dimensionless eroded area (denoted *damage* in the following), given in Equation (2.6).

$$\frac{H_{m0}}{\Delta \cdot D_{n,50}} = \begin{cases} 6.2 \cdot \frac{1}{\xi_{0m}^{-0.5}} \cdot P^{0.18} \cdot \left(\frac{S}{\sqrt{N}}\right)^{0.2} & for\ plunging\ waves \\ \xi_{0m}^{P} \cdot \sqrt{cot(\alpha)} \cdot P^{-0.13} \cdot \left(\frac{S}{\sqrt{N}}\right)^{0.2} & for\ surging\ waves \end{cases} \tag{2.5}$$

$$S = \frac{A_e}{D_{n,50}^2} \tag{2.6}$$

Where:

N	number of waves	$[-]$
P	notional permeability, van der Meer [1988]	$[-]$
S	damage parameter	$[-]$
A_e	eroded area	$[m^2]$
ξ	surf similarity parameter	$[-]$

The formulas are plotted in Figure 2.1, for a damage S=5, permeability P=0.6 and the number of waves N=3000. The curves are plotted for given S, P and N, as well as different front slopes. In this simple plot, the intersection point between the two lines, called the transition point, is clearly visible.

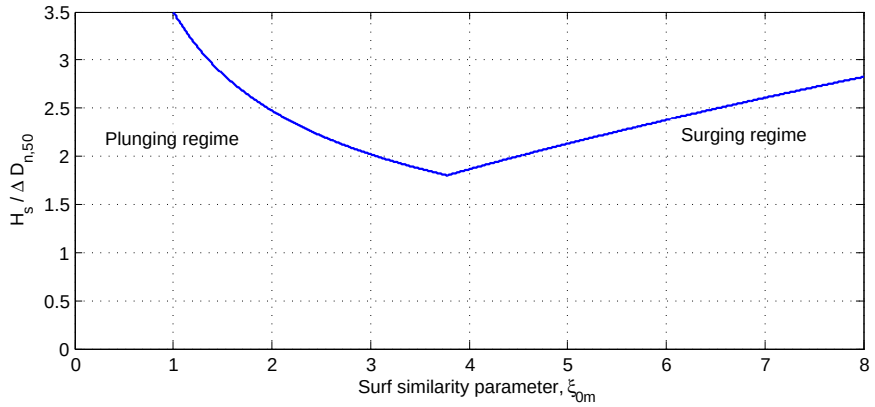

Figure 2.1. Plot of van der Meer formulas.

The point where the curve for plunging waves and the one for surging waves intersect is defined by Equation (2.7).

$$\xi_{0m,cr} = \left(6.2 \cdot P^0.31 \cdot \sqrt{tan\alpha}\right)^{\frac{1}{P+0.5}} \tag{2.7}$$

H_0 does not include the influence of the wave period. van der Meer [1988] indroduces a parameter that accounts for the influence of wave period. This parameter is defined in Equation (2.8).

$$H_0 T_0 = \frac{H_{m0}}{\Delta \cdot D_{n,50}} \cdot \sqrt{\frac{g}{D_{n,50}}} \cdot T_{0,1} \tag{2.8}$$

Where:

g	gravitational acceleration	$[m/s^2]$ *or* $[N/kg]$
$T_{0,1}$	spectral mean wave period	$[s]$

PIANC [2003] defines ranges for the two stability parameters described in this section, for three mobility criteria, as shown in Table 2.1. The regime defines the type of berm breakwater reshaping.

Table 2.1. Mobility criterion (the criterion depends on stone gradation) [PIANC, 2003].

Regime	H_0	H_0T_0
Statically stable non-reshaped berm breakwater	<1.5-2	<20-40
Statically stable reshaped berm breakwater	1.5-2.7	40-70
Dynamically stable reshaped breakwater	>2.7	>70

The article by Lykke Andersen, van der Meer, Burcharth, and Sigurdarson [2012] studies berm breakwaters and the application of the van der Meer foruma in this case. The authors find that predictions using the van der Meer formula for plungin waves fit the data, even in the case of surging waves.

2.2 Van der Meer

van der Meer [1988] consists of an extensive research on the reshaping of berm breakwaters concerning both statically stable and dynamically stable strucures. Drawing from previous studies, and developing new formulas, the author obtains models for reshaping prediction. The models are further developed by van der Meer [1992]. The study is based both on a large set of original data and data from other studies.

The damage level, S, is a nondimensional parameter defined by Equation (2.9), with $S < 3$ being the threshold for "no damage", or "start of damage".

$$S = \frac{A}{D_{n,50}^2} \tag{2.9}$$

Van der Meer compiles a large list of gouverning variables which is condensed by introducing dimentionless variables, like the damage, S, mentioned before. The list of variables for static stability is given in Table 2.2

Table 2.2. Governing variables for static stability [van der Meer, 1988].

Name of variable	Expression	Range
Wave height parameter	$H_s / \Delta \cdot D_{n,50}$	1 - 4
Steepness	s	0.01 - 0.06
Surf similarity	ξ	0.7 - 7
Damage as function of number of waves	$S/\sqrt{N}$	<0.9
Slope	$cot\alpha$	1.5 - 6
Stone grading	D_{85}/D_{15}	1 - 2.5
Permeability	P	0 - 1
Spectral shape parameter	κ	0.3 - 0.9
Crest height	R_c/H_s	(-1) - 2
Front slope angle	$cot(\alpha)$	1 - 5

van der Meer [1992] reanalyzes the research previously done by the same author, and focuses specifically on the case of berm breakwaters in some of the tests. The parameters described earlier are used to develop a computer program, which proves reliable in giving predictions on front slope reshaping when tested against both independently obtained data, and data obtained from other researchers. The computer program generates a predicted profile, as the one shown in Figure 2.2. As the author mentions, the profile is independent of its initial slope, the only parameter determining the profile is the location of the intersection between the profile and the SWL. The relationships between variables and profile parameters are detailed in Appendix B.2.

van der Meer [1992] conducts 16 tests on a berm breakwater with an initial front slope of 1:1.5, with a H_0 range of 3 to 6. The berm level is varied from -0.1 m to 0, and finally +0.1 m.

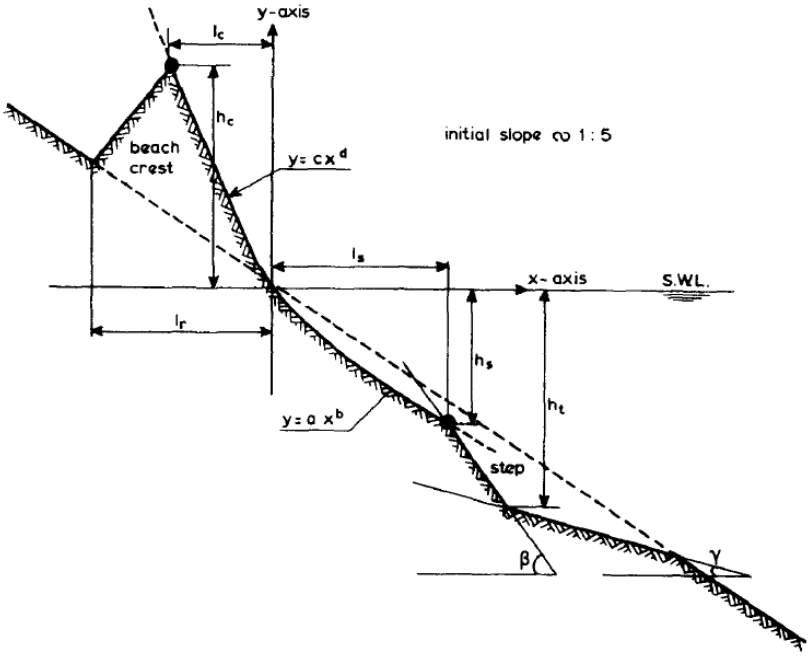

Figure 2.2. Van der Meer's schematized profile [van der Meer, 1992].

2.3 Tørum and Krogh

The method for estimating berm recession is given in Equation (2.11), taken from PIANC [2003]. Tørum and Krogh [2000] is a version of Tørum [1998], that is designed to take more parameters into account (like water depth and gradation of stones). The range of these expressions is given as:

$$12.5 < \frac{d}{D_{n,50}} < 25 \tag{2.10}$$

The formula has been developed for calculating recession for multi-layer berm breakwaters, and can be analyzed in comparison to the case of the Sirevåg berm breakwater in Norway. The test parameters feature a high berm, and limited overtopping.

$$\frac{Rec}{D_{n,50}} = 2.7 \cdot 10^{-6}(H_0T_0)^3 + 9 \cdot 10^{-6}(H_0T_0)^2 + 0.11H_0T_0 - f_{grading} - f_d \tag{2.11}$$

$$f_{grading} = (-9.9f_g^2 + 23.9f_g - 10.5) \tag{2.12}$$

$$f_g = \frac{D_{n,85}}{D_{n,15}} \tag{2.13}$$

$$f_d = -0.16\left(\frac{d}{D_{n,50}}\right) + 4 \tag{2.14}$$

Where:

f_g	gradation factor	$[-]$
f_d	depth factor	$[-]$
d	water depth in front of the breakwater	$[m]$

Equation (2.15) gives the depth h_f, at which the original profile intersects the reshaped profile, as explained in Figure 2.3.

$$\frac{h_f}{D_{n,50}} = 0.2\frac{d}{D_{n,50}} + 0.5 \tag{2.15}$$

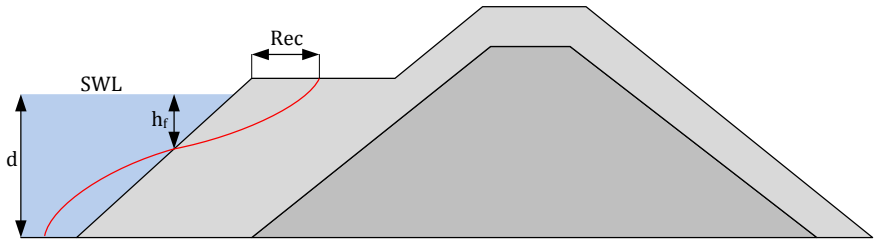

Figure 2.3. Recession and h_f.

2.4 Lykke Andersen

This formula has been developed through conducting a large number of tests at Aalborg University. Due to the large number of tests, and validation against data from model tests conducted by other researchers, this formula can be considered very reliable. This claim is also supported by results.

Lykke Andersen and Burcharth [2009] constructed a berm breakwater model with a homogenous berm, and varied wave steepness, height, period, as well as the geometry of the structure itself, by changing the crest height and berm width. By changing the water depth, the water depth above the berm was varied, inlcuding tests with the water level above the berm. The tests were conducted with various armour sizes, while keeping the same stone size for the core material.

In this article, the influence of the various parameters was studied, with the aim of developing a new recession formula. Wave attack direction was not studied directly, but accounted for by referring to van der Meer [1988]. For the influence of the number of waves, a formula was given, that fitted the data. The number of waves used in the study was 3000. Lykke Andersen and Burcharth [2009] observed that after 500 waves, only minor changes occur in the case of dinamically stable profiles. This number is higher for statically stable profiles.

Stone gradation and shape was accounted for by including a factor in the recession formula, based on earlier studies cited in the article. An exponential function of H_0, the stability index, was introduced to account for its influence. This factor is obtained by studying the data set generated for the article, together with information available from van der Meer [1988].

Finally, the researchers include a factor that accounts for wave characteristics such as H_{m0}, T_m, as well as skewness, based on some earlier work by Lykke Andersen [2006].

The Lykke Andersen formula for the estimation of berm recession is given in Equation (2.16). The detailed formulas and descriptions of the various factors are given in Appendix B.

$$\frac{Rec}{D_{n,50}} = f_{hb} \cdot \left[f_{H0} \cdot \frac{2.2 \cdot h - 1.2 \cdot h_s}{h - h_b} \cdot f_\beta \cdot f_N \cdot f_{grad} \cdot f_{sk} - \frac{|cot(\alpha_d) - 1.05|}{2 \cdot D_{n,50}} \cdot (h - h_b) \right] \tag{2.16}$$

Where:

f_{hb}	berm elevation factor	$[-]$
f_{h0}	stability index factor	$[-]$
f_β	incident wave angle factor	$[-]$
f_N	number of waves factor	$[-]$
f_{grad}	stone gradation factor	$[-]$
f_{sk}	skewness factor	$[-]$
h	water depth at toe	$[m]$
h_s	step height	$[m]$
h_b	water depth above berm	$[m]$
α_d	angle of the front slope	$[^\circ]$

2.5 Moghim

This study attempts to introduce a new formula for recession calculations, based on test results performed at the Iranian National Center of Oceanography. In addition, the researchers introduce a new dimensionless parameter, $H_0\sqrt{T_0}$, based on the assumption that the wave height and period do not have the same order of magnitude when considering their influence on stability. The new parameter is based on the data generated by the conducted experiments, and it impacts on the validity range of the new formulas. Equation (2.17) holds for values of $H_0\sqrt{T_0} < 17$, whilst Equation (2.18) holds for values of $H_0\sqrt{T_0}$ greater than or equal to 17. The equations are valid within the limits defined in Table 2.3. The new parameter introduced in these formulas is h_{br}, which is the berm eleveation above SWL.

For $H_0\sqrt{T_0} < 17$:

$$\frac{Rec}{D_{n,50}} = \left(10.4 \cdot \left(H_0\sqrt{T_0}\right)^{0.14} - 13.6\right) \cdot \left(1.61 - exp\left[-2.2 \cdot \frac{N}{3000}\right]\right) \cdot \left(\frac{h_{br}}{H_s}\right)^{-0.2} \cdot \left(\frac{d}{D_{n,50}}\right)^{0.56} \tag{2.17}$$

For $H_0\sqrt{T_0} \geq 17$:

$$\frac{Rec}{D_{n,50}} = \left(0.089 \cdot H_0\sqrt{T_0} + 0.49\right) \cdot \left(1.61 - exp\left[-2.2 \cdot \frac{N}{3000}\right]\right) \cdot \left(\frac{h_{br}}{H_s}\right)^{-0.2} \cdot \left(\frac{d}{D_{n,50}}\right)^{0.56} \tag{2.18}$$

Table 2.3. Validity ranges for Moghim et al. [2011].

Parameter	Low	High
$H_0\sqrt{T_0}$	7.7	24.4
N	500	6000
h_{br}/H_S	0.12	1.24
$d/D_{n,50}$	8.0	16.5
d/L	0.09	0.25
f_g	1.2	1.5

2.6 Shekari

A formula which includes the influence of wave height and period, number of waves and berm height is developed by Shekari and Shafieefar [2012]. This recent formula is distinguishable by the inclusion of berm width into calculations. The formula is shown in Equation (2.19).

$$\frac{Rec}{D_{n,50}} = \left[-0.016 \cdot (H_0\sqrt{T_0})^2 + 1.59 \cdot H_0\sqrt{T_0} - 9.86\right] \cdot \left[1.72 - exp\left(-2.19 \cdot \frac{N}{3000}\right)\right] \cdot \left(\frac{B}{D_{n,50}}\right)^{-0.15} \cdot \left(\frac{h_{br}}{H_s}\right)^{-0.21} \tag{2.19}$$

Shekari and Shafieefar [2012] uses a berm breakwater with a front slope of 1:1.25, which in the study is considered close to the natural angle of response of the stones. The reshaping of the breakwater is measured using a point gauge in three crosssections of the structure, with measurements made with a 1 cm spacing. The mean of the three profiles is used to calculate recession. A total of 222 tests are carried out. The ranges studied by Shekari and Shafieefar [2012], which can be considered the validity ranges of the formula are given in Table 2.4.

The parameter $H_0\sqrt{T_0}$, previously intorduced by Moghim et al. [2011], is used in the formula, and the study concludes that its use in the estimation of berm recession is appropriate.

Table 2.4. Validity ranges for Shekari and Shafieefar [2012].

Parameter	Low	High
$H_0\sqrt{T_0}$	7.09	23.52
N	500	6000
h_{br}/H_S	0.22	1.57
$d/D_{n,50}$	9.6	14.11
$B/D_{n,50}$	14	29.41

Focusing on the effect of the berm width on stability, the main conclusion is that the recession increases inversely proportional to the berm width. This statement is based on tests conduted with 5 different berm widths.

2.7 Comparison of current recession estimation methods

A comparison of several recession formulas has been made by Tørum, Moghim, Westeng, Hidayati, and Øivind Arntsen [2011]. The Lykke-Andersen formula can be considered the most versatile, as it includes the most parameters and has the widest validity range for those parameters. The Tørum formula has been derived for multi-layer berm breakwaters, such as the Sirevåg berm breakwater in Norway. The Sirevåg breakwater, shown in Figure 2.4, is a well-studied case in the literature. The construction and use of this berm breakwater, as well as it being subjected to the design storm, provided useful data for researchers.

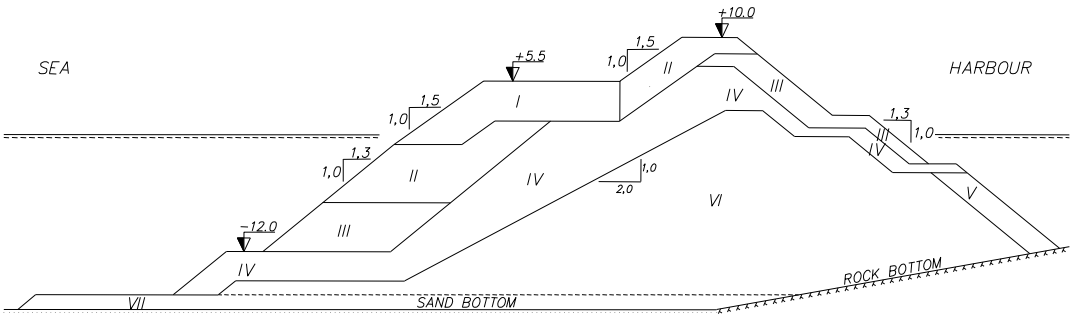

Figure 2.4. Sirevåg berm breakwater [Sigurdarson et al., 2003].

When looking at the stability parameter H_0T_0, it can be said that, for values of H_0 larger than 5, it is the governing recession parameter. In the cases of low H_0, the wave period seems to have less influence than the one taken into account by H_0T_0. This consideration is taken into account by Moghim et al. [2011], by introducing the stability parameter $H_0\sqrt{T_0}$, as it will be discussed later.

Of the studies mentioned in this chapter, Lykke Andersen and Burcharth [2009] takes into account the initial front slope. *BREAKWAT*, the program developed after van der Meer [1988] and van der Meer [1992] also takes into account the initial front slope when predicting the reshaped profile.

Part II

Model testing

3 Test plan

As resulted from the problem analysis, there are a number of variables which are considered in the different studies listed. To reach the aim of this project, an experiment is conceived. This chapter identifies the parameters that will be varied during the planned tests, and will establish a test programme.

3.1 Test parameters

The most important parameters for the reshaping of berm breakwaters are the sea states and stability parameters. Additionally, different formulas use different other parameters such as the front slope and berm elevation. This section comments on the parameters chosen for testing in this report and discusses their relevance.

In this section the equivalent cubic length, $D_{n,50}$ will be referenced. As it will be detailed later in the report, the value of the equivalent cubic length of the armor stones used in the tested configurations is $D_{n,50} = 0.0317m$.

Front slope

The slope ranges found in Icelandic type berm breakwaters are 1:1.25 to 1:1.5. Initially they were build with a steep slope, such as 1.1. As the concept has been developed, the slopes became more gentle, in the ranges of 1:1.3 to 1:1.5. This increase in the slope leads to a very stable berm [Sigurdarson, Smarason, Voggosson, and Bjørdal, 2006]. Also, as suggested by the same researchers, an S-shaped profile with two slopes can be used. Although this design increases stability, it is more difficult to build. For this report, two straight front slopes will be used: 1:1.1 and 1:1.5.

Steepness

Steepness is an indication of the relationship between the height of a wave, H and its length L. When an analysis is performed using the mehtod of Van der Meer, steepness is an important factor. In this report, 5 steepnesses will be used: 1%, 1.5%, 2%, 3%, and 4.5%.

$$s_{0m} = \frac{H_{m0}}{L_{0m}} \tag{3.1}$$

Reynolds number and scale effects

Scale effects are studied in relation to the Reynolds number, given in Equation (3.2). van der Meer [1988] researches the scale effects and gives a reference range for the Reynolds number, $Re = 1 \cdot 10^4$ to $4 \cdot 10^4$, over which scale effects can be considered minimum.

$$Re = \frac{\sqrt{g \cdot H_s}}{\nu} \cdot D_{n,50} \tag{3.2}$$

Where:

$$\nu \mid \text{kinematic viscosity for water} \quad [m^2/s]$$

For the current study, the lowest Reynolds number, for $H_s = 0.064[m]$ and $D_{n,50} = 0.0317$, is $Re = 2.501 \cdot 10^4$. The range of values for Re can be found in Table 3.1.

Stability parameters

Wave height is an important factor for calculating stability parameters. Increasing the wave height will change weather the analysed case can be considered statically stable or dynamically stable. For each steepness considered, a wave height of 0.064 m will be used, and increased subsequently for the following tests to 0.097 m, 0.131 m, and 0.164 m. For a description of wave run-up and run-down, which are key aspects influenced by wave height, refer to Appendix A. Stability parameters used in testing are H_0 and H_0T_0, described in Section 2.1. As can be seen in Table 3.1, while considering what is discussed in Section 2.1, most tests fall within the category of statically stable berm breakwaters both when looking at the H_0 parameter, and the H_0T_0 parameter.

Ranges of parameters for model testing are presented in Table 3.1.

Table 3.1. Parameter ranges.

Name	Symbol	Unit	Range
Steepness	s_{0m}	-	0.015 - 0.045
Wave height	H_s	m	0.064 - 0.164
Stability parameter	H_0	-	0.8 - 2.1
Stability parameter	H_0T_0	-	11.6 - 88.5
Reynolds number	Re	-	$2.5 \cdot 10^4 - 4 \cdot 10^4$
Berm elevation	h_{br}	m	0.04 - 0.07

Berm elevation

The berm elevation above SWL is denoted here h_{br}. This is the same concept as the water depth above berm h_b, i.e., h_{br} is always equal to $-h_b$. The berm elevation is an important variable in many of the formulas considered in this report, and therefore the berm height will be varied. The two values for h_{br} are 0.04 cm and 0.07 cm.

3.2 Test programme

Considering the variables listed in Section 3.1, a test programme is devised using five configurations: a berm breakwater with $h_{br} = 0.04m$ with front slopes of 1:1.1, 1:1.25 and 1:1.5, a straight slope (no berm) of 1:1.5, a berm breakwater with a berm at $0.07m$ above SWL with a front slope of 1:1.1. Table 3.2 shows the different configurations planned for testing.

Table 3.2. Configurations and test names.

Test names	Front slope [-]	h_br [m]	No. of tests	Observations
1xx	1:1.1	0.04	19	-
2xx	1:1.5	0.04	19	-
3xx	1:1.25	0.04	5	progressing errosion
5xx	1:1.5	-	6	no berm, straight slope
6xx	1:1.1	0.07	6	-

After the test setup is complete, including the installation of the profiler, wave gauges and the construction of the model, the following test procedure is abode:

1. A scan of the initial profile is taken.
2. The flume is filled to the prescribed level and the absorbtion system is calibrated.
3. The wave gauges are calibrated.
4. Irregular waves are generated according to the test programme.
5. The water is pumped out of the flume and the final profile is scanned.
6. The results are verified for accuracy and a reflection analysis is performed.
7. The structure is rebuilt.

Figure 3.1 shows the planned seastates for each front slope tested. Note that no test is run for wave height 0.164 in the case steepness 0.01, so test 154 is missing from both the table and figure. This omission is made because of the unusual length of the waves obtained and the limitations of the wave generator.

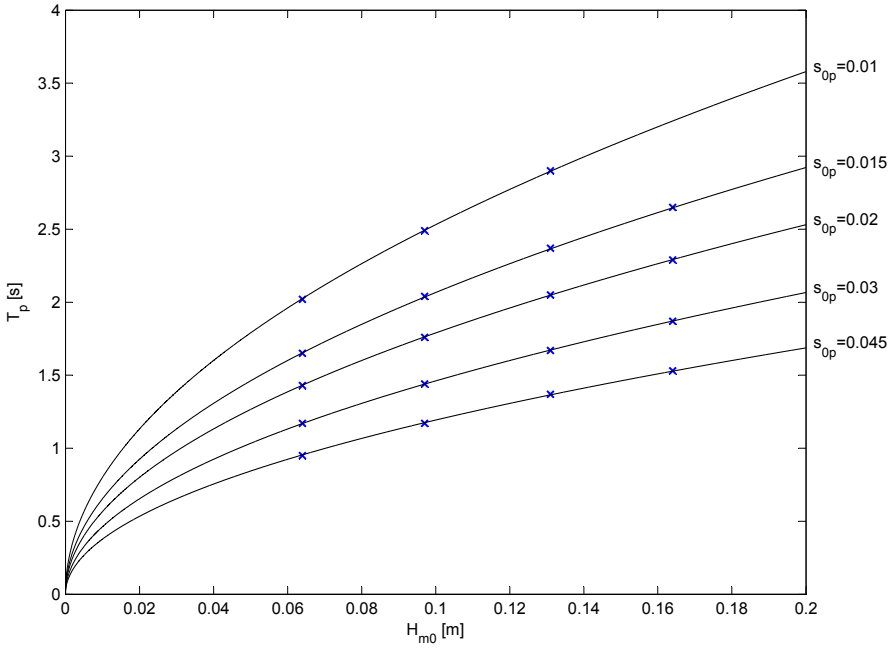

Figure 3.1. Planned seastates.

A sample of the proposed test programme, for a front slope of 1:1.1 is presented in table 3.3. The full test programme is found in Appendix C.

Table 3.3. Program for model testing. First configuration.

Test Name	s_p [-]	H_s[m]	H_0[-]	T_p[s]	H_0T_0[-]
111	0.015	0.064	0.8	1.65	21
112		0.097	1.3	2.04	42.2
113		0.131	1.7	2.36	63.8
114		0.164	2.1	2.65	88.5
121	0.02	0.064	0.8	1.43	18.2
122		0.097	1.3	1.77	36.6
123		0.131	1.7	2.05	55.4
124		0.164	2.1	2.29	76.5
131	0.03	0.064	0.8	1.17	14.9
132		0.097	1.3	1.44	29.8
133		0.131	1.7	1.67	45.1
134		0.164	2.1	1.87	62.4
141	0.05	0.064	0.8	0.91	11.6
142		0.097	1.3	1.12	23.2
143		0.131	1.7	1.29	34.9
144		0.164	2.1	1.45	48.4
151	0.01	0.064	0.8	2.02	11.6
152		0.097	1.3	2.49	23.2
153		0.131	1.7	2.90	34.9

4 Model details and construction

This chapter will describe the materials used in the construction of the breakwater model and illustrate its dimensions. The parameters that define the stones used are:

W_{50}	median weight	$[kg]$
ρ_s	mass density of stones	$[kg/m^3]$
$D_{n,50}$	equivalent cube length	$[m]$

These parameters and their importance are discussed in Section 2.1. The equivalent cube length is obtained from the median weight of stones and their mass density using Equation (2.3). W_{50}, ρ_s, and $D_{n,50}$ are determined by measuring the properties of 150 stones.

The material specifications for the core and armour stones are given in Table 4.1.

Table 4.1. Stone specification.

Parameter	Armour	Core
W_{50}	0.0874	0.0069
ρ_s	2743	2700
$D_{n,50}$	0.0317	0.0137

Figure 4.1 shows the grain size distribution curves for the armour stones used in this experiment. Note that the units used for the grain size distribution are milimeters and in the figure that illustrates the non-dimensional cubic length, the x-axis does not start from 0.

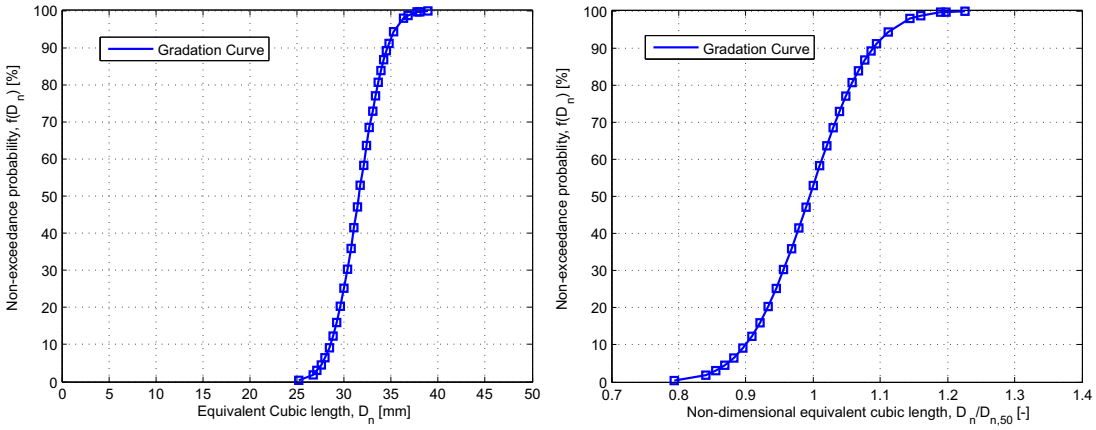

Figure 4.1. **Left:** Grain size distribution. **Right:** Nondimensionalization of size distribution function.

4.1 Model dimensions

In order to test the influence of different parameters, tests are run in five different configurations.
The model dimensions are illustrated below, in Figures 4.2, 4.3, 4.4 and 4.5.

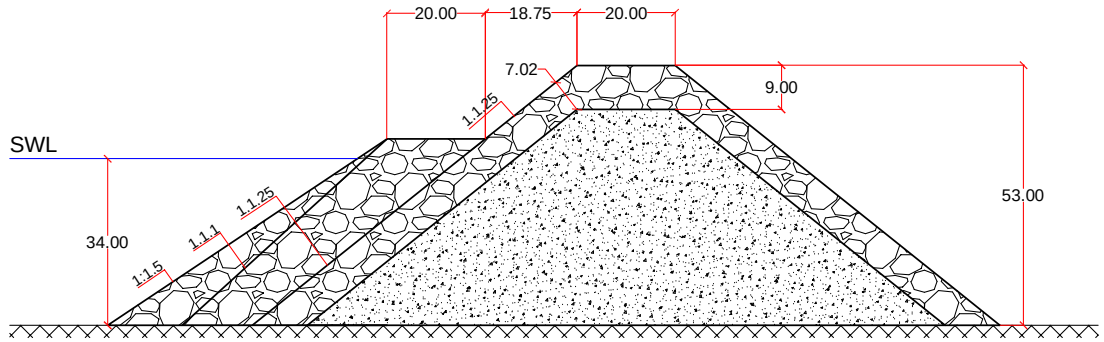

Figure 4.2. Berm breakwater: Dimensions for *lowberm* tests.

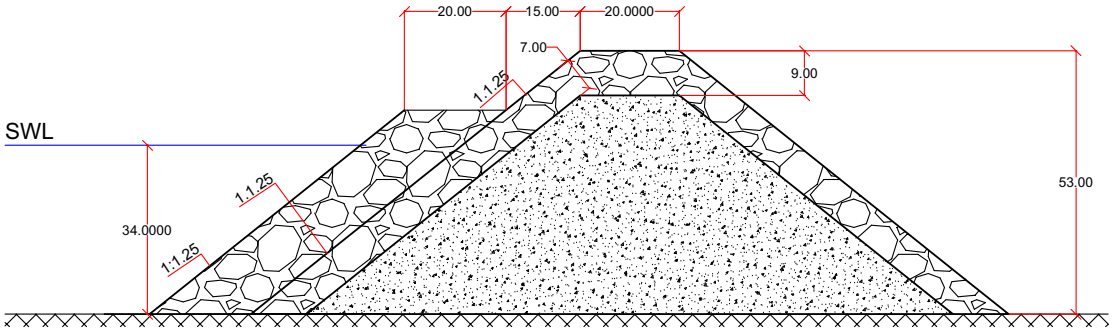

Figure 4.3. Berm breakwater: Dimensions for *progressive errosion* tests.

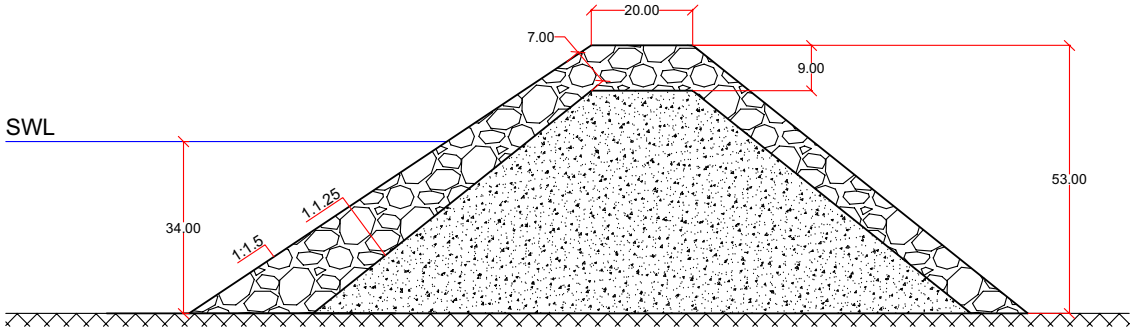

Figure 4.4. Berm breakwater: Dimensions for *straight slope* tests.

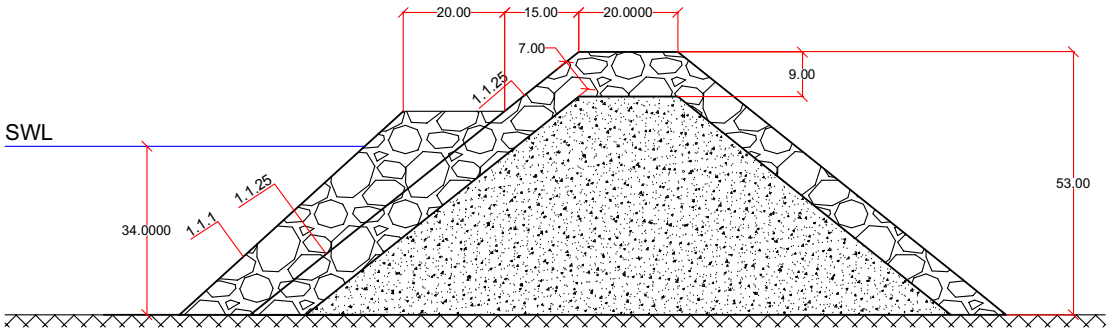

Figure 4.5. Berm breakwater: Dimensions for *high berm* test.

5 Equipment and measurements

This chapter will give a description of the equipment used to collect data. This equipment includes the wave gauges, non-contact erosion profiler and overtopping measuring equipment.

Erosion profiler

The initial and reshaped profiles of the berm breakwater are obtained by making non-contact measurements in 3-D. These measurements are made using a laser controled by a computer running *EPro*, a computer program developed at Aalborg University specially for this purpose. Figure 5.1 shows the hardware that performs the scan [Meinert, 2006]. The green arrows indicate the axis on which the machine moves.

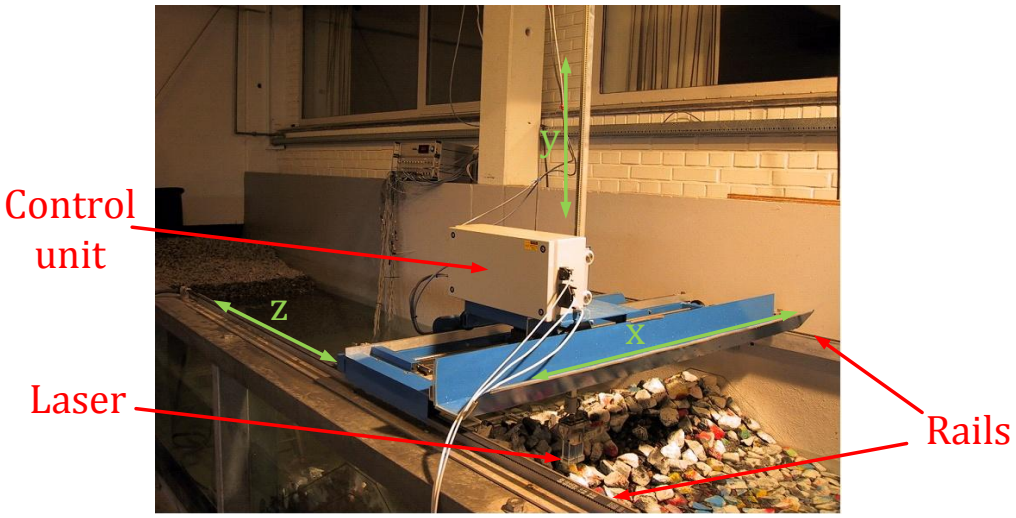

Figure 5.1. Non-contact profiling of a breakwater.

EPro allows for the selection of a scan pattern. This function is useful in conjunction with another capability of the program, called *surround distance*. When the laser cannot get a reading, the program uses an average of the surrounding measurements to provide an estimate. A surround distance is input by the researcher.
The selected pattern has the advantage of not having to readjust on the y-axis during a sweep, thus increasing accuracy and scanning time. Furthermore, if the laser fails to scan a certain point, the averaging function of the program can be applied.

Measuring overtopping

Overtopping is measured by collecting the water overtopping a 30.5 cm section of the model. The water is collected in an tank located behind the breakwater and a pump is used to lead the water from the overtopping chamber to a container outside the flume. The quantity of water is then measured by weight. In Figure 5.2 the profile of the breakwater is shown together with the positioning of the collector and overtopping tank.

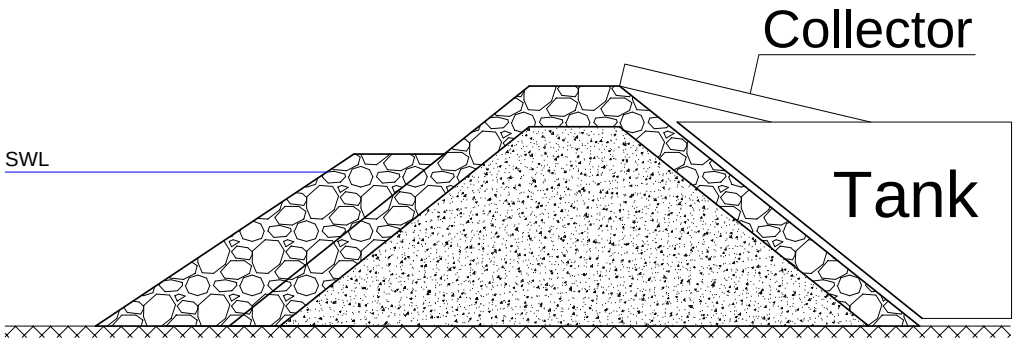

Figure 5.2. Berm breakwater overtopping chamber.

5.1 Flume setup

The model used for the experimental part of the project was tested in the Shallow Water Wave Flume at the Hydraulics and Coastal Engineering Laboratory of Aalborg University. The flume has a length of 25 m, 1.5 m width a depth of 1 m.

For the wave generation, the flume is equipped with a piston-type wave generator. To prevent the apparition of cross-waves, porous walls were mounted in the flume as it is illustrated in the figures below. The waves reflected by the model are damped by the active absorption system of the generator, based on data coming from a series of wave gauges next to the paddle of the generator.

In Figure 5.3 and Figure 5.4 the flume setup is shown with the position of the breakwater, wave gauges, porous walls and wave generator.

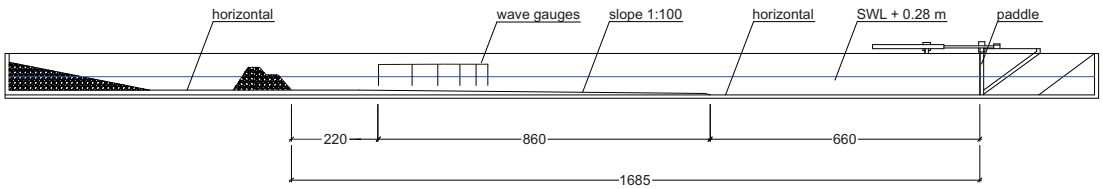

Figure 5.3. Flume setup for the tests. Longitudinal view. (annotations in [mm])

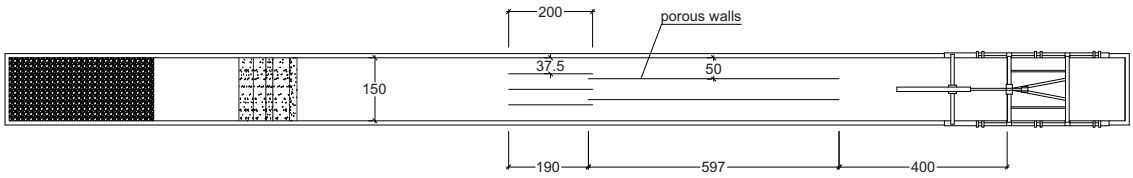

Figure 5.4. Flume setup for the tests. Top view. (annotations in [mm])

5.2 Wave gauges position

As illustrated in Figure 5.3, there is a certain upward slope in the flume from the wave generator until the position of the breakwater model. The height of the waves

is influenced by this slope and so, wave gauges are mounted in the flume to measure this effect and assure that the waves over the breakwater are the desired ones.

The wave gauges are able to record the wave heights passing through the flume and also separate the incident wave heights from the reflected ones. To have reliable recordings, the wave gauges are positioned according to Mansard and Funke [1980], where the influence the positioning of the wave gauges has over the data reliability is investigated.

Shoaling

The bottom of the flume has a certain slope, the effect this slope has over the waves is called *shoaling*. Shoaling is the two dimensional phenomenon that occurs as the waves propagate from deeper to more shallow water, e.g., when the wave is approaching the coast. Both the wave heights and wave lengths are affected by this phenomenon. As the wave moves along a certain slope, it's height will keep increasing while it's length is being reduced, thus an increase in wave steepness is being developed. This process will continue until the wave will become unstable and break. It is important to say that the wave period remains constant through the process.

The shoaling coefficient is defined as the wave height at the target location divided by the wave height at the measurement location. This process is taken into account during the testing in the laboratory by specifying to the wave generator, located at deeper water, to generate waves of certain height and length that, when they arrive at the breakwater, will have the desired parameters.

Gap between wave gauges

The selection of the distance between wave gauges is important for recording the incident wave height and the separation of the incident and reflected spectrum. *WaveLab* allows the selection of different methods of reflection analysis, of which the following are considered for this report: Mansard and Funke [1980], Zelt and Skjelbreia [1992] or Grønbech, Jensen, and Andersen [1996]. The methods proposed by Zelt and by Grønbech allow the use of multimpe gauges. However, according to Mansard and Funke prescriptions, three gauges are needed, with precise spacing.

Mansard and Funke [1980] gives the following recommendations for the gaps between wave gauges, when performing a reflection analysis:

$$x_{1,2} = \frac{L_p}{10} \tag{5.1}$$

$$\frac{L_p}{6} < x_{1,3} < \frac{Lp}{3} \tag{5.2}$$

$$x_{1,3} \neq \frac{L_p}{5} \tag{5.3}$$

$$x_{1,3} \neq \frac{3 \cdot L_p}{10} \tag{5.4}$$

$x_{1,2}$ is the distance between the first and second wave gauges, and $x_{1,3}$ is the distance between the first and third gauges selected for reflection analysis. Considering the

range of wavelengths, L_p, tested, a large number of wavegauges is necessary. For this experiment, 6 gauges are mounted in the configuration shown in Figure 5.5. Note that the figure is not to scale. A complete and scaled drawing of the wave gauges positions inside the flume is given in Figure 5.3.

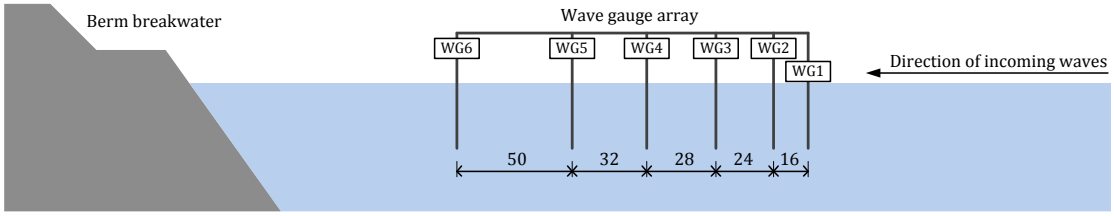

Figure 5.5. Chosen wavegauge configuration. Distances measured in cm.

To perform a reflection analysis using the method described earlier, three gauges are selected according to the aforementioned criteria. For example for a wave length of L_p=8.4 m, $x_{1,2} = 0.84\ m$, $1.4\ m < x_{1,3} < 2.4\ m$, $x_{1,3} \neq 1.68\ m$ and $x_{1,3} \neq 2.52\ m$. This means that gauges WG2, WG4 and WG6 may be chosen, or alternatively WG1, WG3 and WG6.

Zelt and Skjelbreia [1992] is an extension of the 3 - gauge system described above, in which all 6 gauges can be used. When analyzing with Grønbech et al. [1996], the *Cross Mode Separation* function in *WaveLab* is used.

Wave generation

WaveLab was used for recording the experimental data. This program was developed at Aalborg University with the purpose of data acquisition and analysis in wave laboratories. The chosen power spectrum for irregular waves is JONSWAP (JOint North Sea WAve Project), which is typically used for seas with limited fetch. The peak enhancement parameter, γ, was chosen as 3.3.
The wave gauges were calibrated before each test, the calibration functions were added for all the channels needed. The wave gauges were calibrated at 2 different water depths, providing liniar calibration functions.

6 Overview of test results

A total of 55 tests were performed. Of those, 19 tests with a front slope of 1:1.1, 19 tests with a front slope of 1:1.5, 6 tests with a straight front slope, at 1:1.5, and 6 tests with a front slope of 1:1.1, with a berm elevation of 7 cm and also 5 tests were done to check damage accumulation.

The obtained sea states are illustrated in Figure 6.1. The figure shows that the researchers were successful in obtaining the necessary sea states. The maximum obtained steepness was 0.0381, and the minimum 0.0078. This data was acquired using *WaveLab*, as detailed in this chapter, in Section 6.

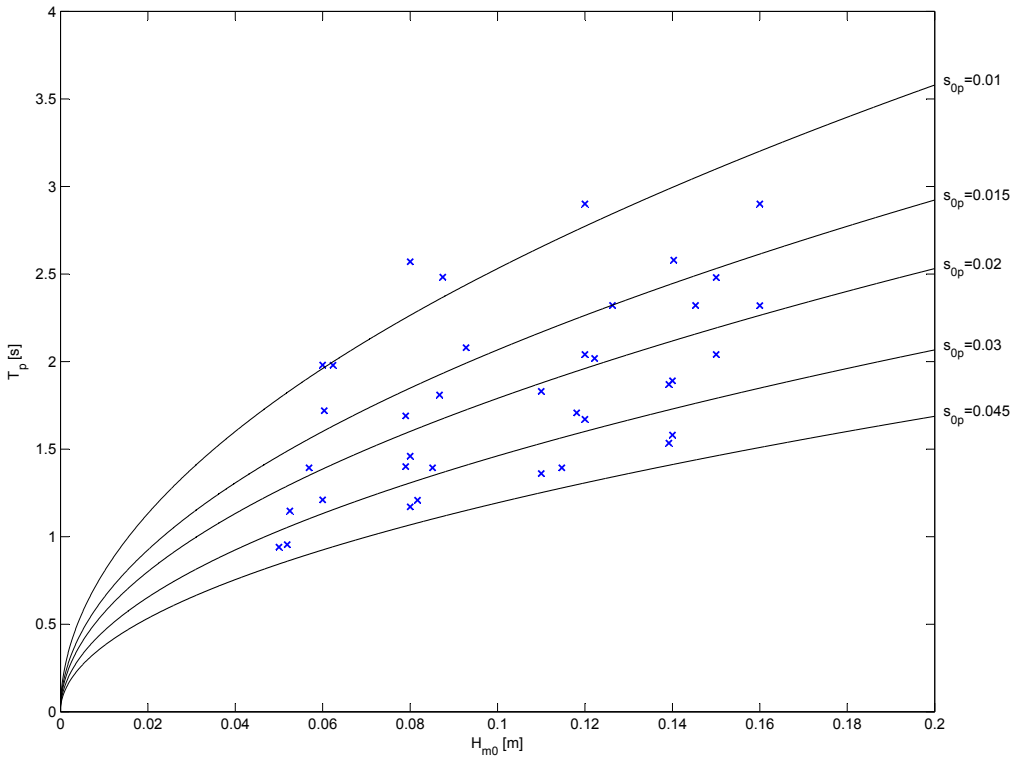

Figure 6.1. Tested seastates.

Wave analysis

Wave analysis is performed for each test recording; from it the frequency domain and time domain wave-parameters are found. *WaveLab* is also used for the separation of incident and reflected waves. Both Zelt and Skjelbreia [1992] and Grønbech et al. [1996] are used in the analysis, providing very similar results, with good reliability. Less than good reliability, resulting from an insufficient number of data points, is found only for a couple of tests with short duration. These are the tests where the profile developed quickly and the test had to be stopped due to full berm recession. Figure 6.2 shows an example of reflection analysis done using *WaveLab*.

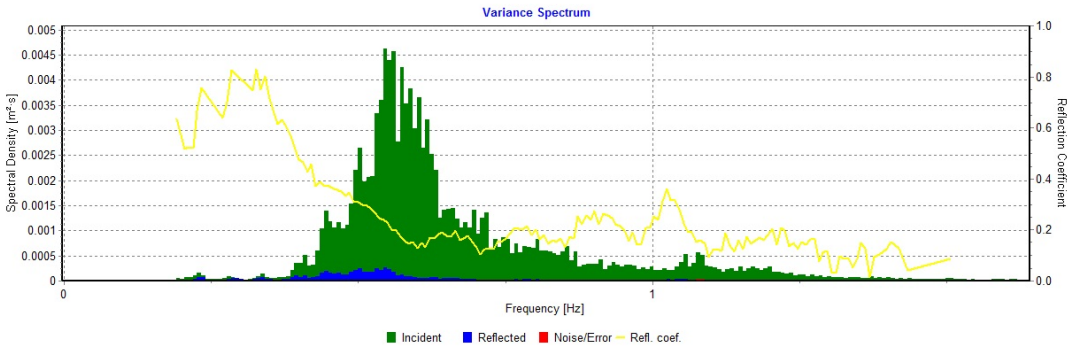

Figure 6.2. Example of a JONSWAP spectrum for an irregular waves test.

Damage detection

EPro is the name of the software used to process the signal from the erosion profiler. This software is also used to control the profiler and set the parameters of the scan, such as speed and acceleation of the scanner, and a scanning grid.

The spacing between grid points was chosen by the reasearchers as 1 cm, to ensure at least one reading for each stone. Spacing higher than 1 cm are expected to yield innacurate results, because of the relatively large $D_{n,50}$ of the stones. This is confirmed by the higher error signal recorded by the profiler. Smaller spacing than the one chosen would increase the time needed for a scan, while bringing no discernible advantage, as 3 or more readings would be expected off the same stone.

Some tests were conducted in order to determine the optimum speed of the scan. *EPro* allows the selection of various speeds and accelerations. The higher speeds decrease the scanning time, but create large error signals, while smaller speeds lead to decreased error signals. An optimal speed was found in the lower range of available speeds, below which the average error signal did not decrease significantly.

The width of the model, equal to the width of the flume, is 1.5 meters. An area of 1.11 m in width, and 1.45 m in length is covered by the scan, meaning that the sections closest to the walls are ignored, thus discarding any influence of the flume walls. A pair of 3D charts scanned by *EPro*, initial and final, are shown in Figure 6.3.

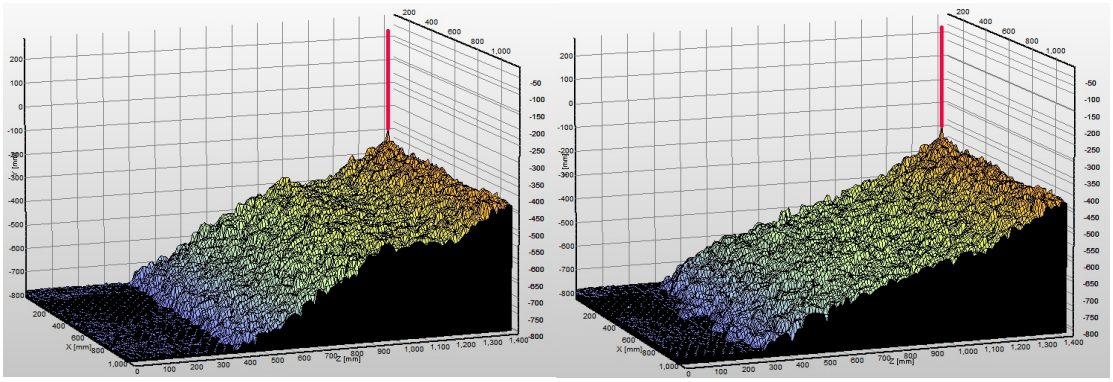

Figure 6.3. 3D surface charts for Test 234.

The results given by the profiler are in the form of a matrix containing the elevations registered at the grid points. This matrix contains 16095 values arrranged in 111 colums and 145 rows. To conduct the analysis, an average profile was obtained for each scan by averaging the 111 crossections. This was done for both initial and final profiles. Figure 6.4 shows an example of a pair of such profiles.

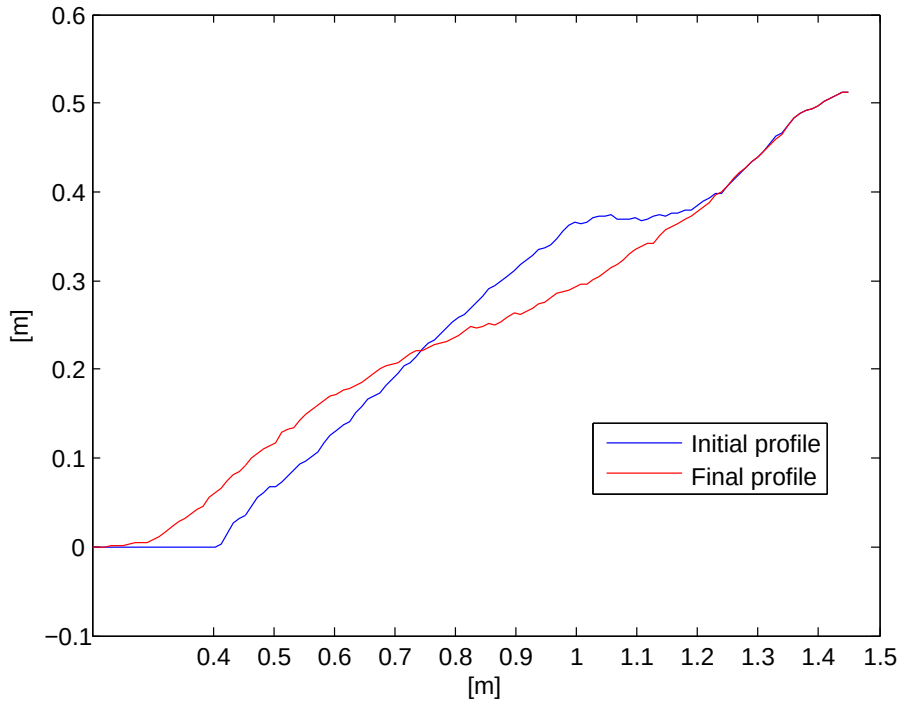

Figure 6.4. Example of reshaped profile, Test 234.

Part III

Results and discussion

7 Stability

The van der Meer stability formulas are investigated in Section 2.1 of this report. Here, the formulas are plotted, but on the vertical axis, the stability parameter is further divided by $(S/\sqrt{N})^{0.2}$. The results are plotted in Figure 7.1. The formulas for the plunging regime are independent of the initial front slope. Consequently, as it can be seen in the figure, the lines for plunging waves overlap. Table 7.1 can be used to clarify the figure.

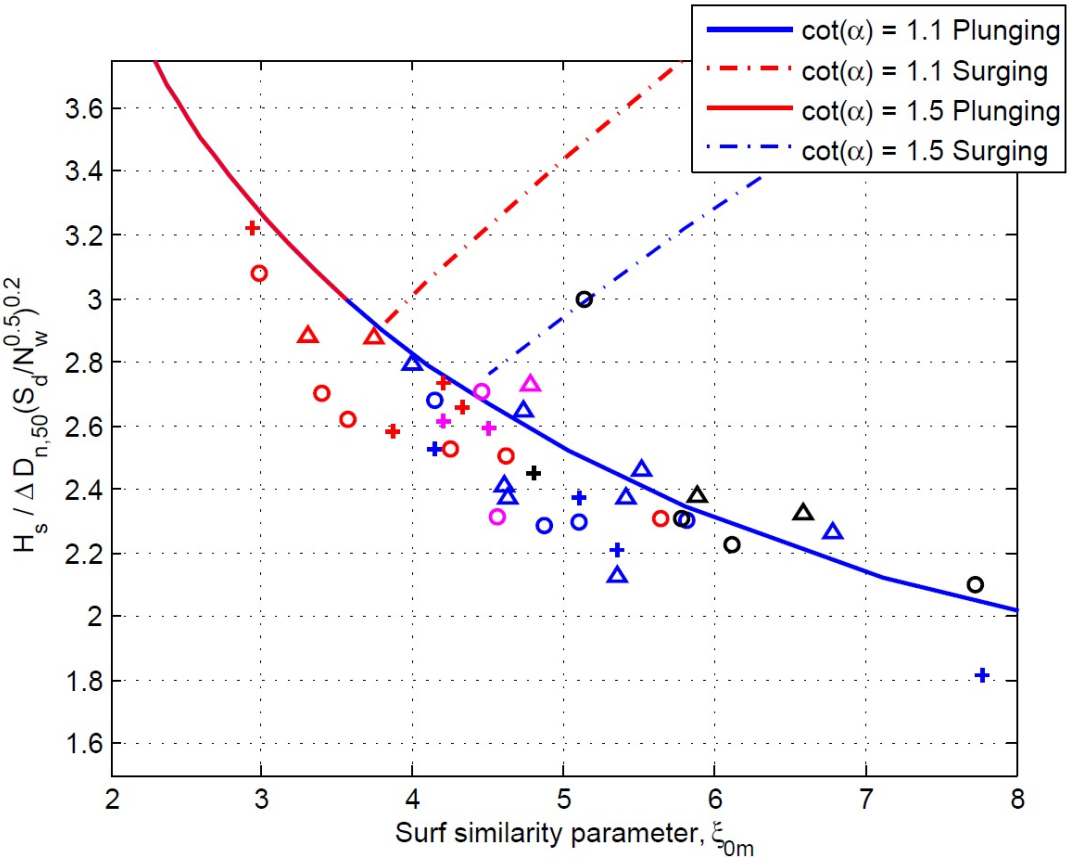

Figure 7.1. Plot of the van der Meer formulas.

Table 7.1. Symbol convention, legend for Figure 7.1.

Damage interval:	$1 < S < 8$	$8 < S < 15$	$15 < S$
$cot(\alpha) = 1.1$, $h_b = -0.04[m]$	○	+	△
$cot(\alpha) = 1.5$, $h_b = -0.04[m]$	○	+	△
$cot(\alpha) = 1.1$, $h_b = -0.07[m]$	○	+	△
$cot(\alpha) = 1.5$, no berm	○	+	△

The formulas predict increased stability with increasing surf similarity parameter, ξ, after a certain transition point. However this is not what the results show. It can be seen that the formula for plunging waves predicts the results found in the surging range. No transition point is identified on the graphs. These findings are consistent with the ones of Lykke Andersen et al. [2012]. The van der Meer formulas are derived

for straight slopes. In the case of berm breakwaters, the presence of the berm might cause a different type of breaking on the sturcture, causing the waves to be plunging even for higher Iribarren numbers. Lykke Andersen et al. [2012] also mentiones the effect of the lack of interlocking stones above the berm elevation. This effect consists of decreased stability.

Specifically to test this formula, a series of 6 tests with a straight slope where designed. However, as can be seen in Figure 7.1, the results are inconclusive. The reason for this is the narrow range of ξ of these tests, and their limited number.

As a conclusion, the stability is found to decrease with increasing ξ, or decreasing steepness, confirming the results of previous studies. For a more detailed view of the test results, in Figure 7.2, the tests are separated depending on the angle of the front slope. The symbol convention from Table 7.1 applies here as well.

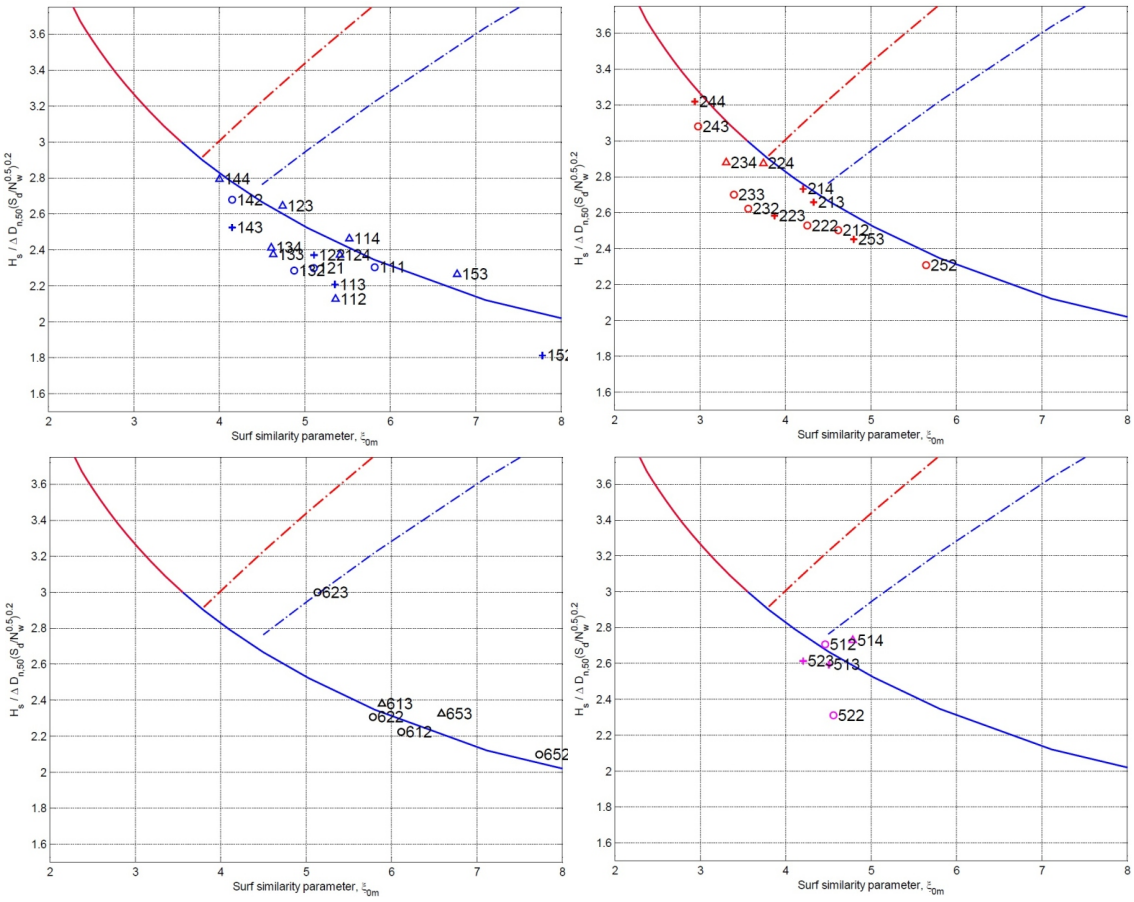

Figure 7.2. Test Comparison.

It can be concluded that the results fit well the formulas for both plunging and surging waves. A small difference is noted, which could be due to the permeability which was not determined for breakwater model. A value of $P = 0.6$ was used for the results shown in Figures 7.1 and 7.2, following Lykke Andersen et al. [2012] and Lykke Andersen [2006]. An improvement has been observed when the permeability was lowered to $P = 0.45$; this is illustrated below, in Figure 7.3.

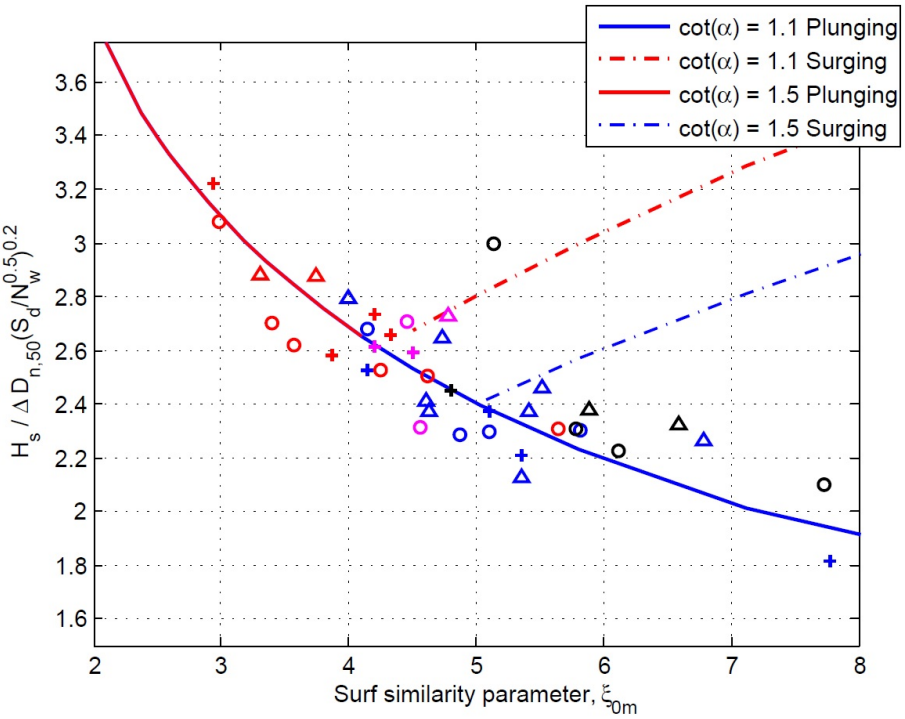

Figure 7.3. Plot of the formulas with $P = 0.45$.

The limits of notional permeability are determined by van der Meer [1988] as 1 for a structure with an impermeable core, and 0.6 for a homogenous structure. Because of the coarse core material used in building the breakwater model, for the present research a value of $P = 0.6$ was used. The change in permeability produced a noticeable change in results in Figure 7.3. This might indicate that, although the core material was considered permeable, the assumption of $P = 0.6$ might have been understated.

7.1 The $H_0\sqrt{T_0}$ stability parameter

A new stability parameter, $H_0\sqrt{T_0}$, is introduced by Moghim et al. [2011]. This is a dimensionless parameter that evaluates the effects of wave height and wave period together. Moghim et al. [2011] argues on the proportionality of the dimensionless berm recession to the newly introduced stability factor. A verification is done by first making the measured recession non-dimensional, as in Equation (7.1).

$$Rec_{DM} = \frac{Rec}{D_{n,50}} \cdot \left(\frac{h_{br}}{H_s}\right)^{0.2} \tag{7.1}$$

The next step is to plot this parameter against the newly introduced stability parameter. This is done in Figure 7.4.

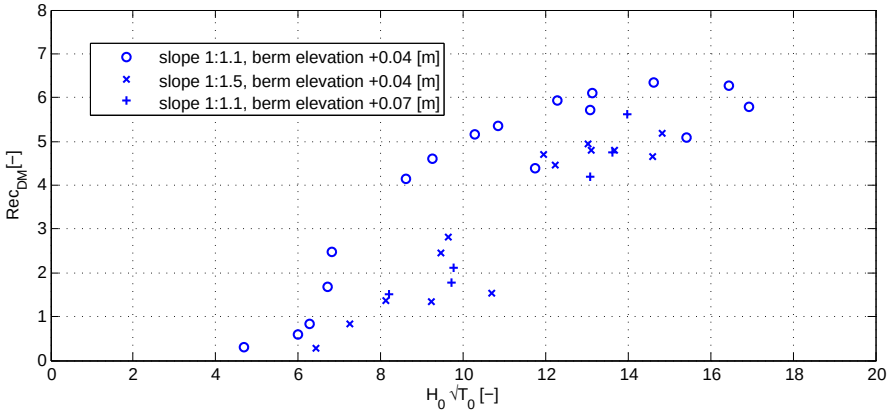

Figure 7.4. Influence of parameter $H_0\sqrt{T_0}$ on berm recession.

By evaluating the plotting of the present data using the method described above, the linear dependency is confirmed, although some scatter is noticed.

8 Berm errosion

This chapter consists of a comparison between the current test results and the calculated recessions using different berm recession formulas. Firstly, the performance of the formulas in predicting the results will be evaluated. Subsequently, some parameters from these formulas will be evaluated and changes will be suggested, when needed, for the ultimate purpose of improving the prediction capability. Finally, a comparison will be made. Each formula will be designated a name that will be used throughout this chapter.

8.1 Evaluation using existing recession estimation methods

In this section, the results will be compared to the predictions obtained by applying the following methods:

- The Lykke-Andersen formula [Lykke Andersen and Burcharth, 2009];
- The Moghim method [Moghim et al., 2011];
- The van der Meer method [van der Meer, 1992];
- The Tørum formula [Tørum and Krogh, 2000];
- The Shekari method [Shekari and Shafieefar, 2012];

The prediction methods mentioned in this chapter have been presented in Chapter 2. Each formula will be evaluated against the present data, bearing in mind the range of application and validity of each formula. Analysis of specific parameters of the formulas will be conducted at a later stage of this paper.
For the purpose of simplification, the following color and shape code is used in plots found throughout this section:

Table 8.1. Symbol convention for recession estimation.

Berm elevation:	$0.04[m]$	$0.04[m]$	$0.07[m]$
Front slope:	1:1.1	1:1.5	1:1.1
Lykke-Andersen	○	△	+
Moghim	○	△	+
van der Meer	○	△	+
Tørum	○	△	+
Shekari	○	△	+

Additionally, the terms *steep slope* and *flat slope* will be used when reffering to $1:1.1$ front slope and $1:1.5$ front slope respectively. The term *high-berm* will be used for the cases of berm elevation $h_{br} = 0.07[m]$, and the term *low-berm* for the situations with $h_{br} = 0.04[m]$.

8.1.1 The Lykke-Andersen recession formula

A validation is made using the Lykke-Andersen recession formula that has been presented in Section 2.4. In Figure 8.1, the measured recession is made dimensionless and is plotted together with the predicted dimensionless recession given by the Lykke-Andersen formula. Aditionally, the 90% confidence bands are plotted, following the Equations (8.1) and (8.2).

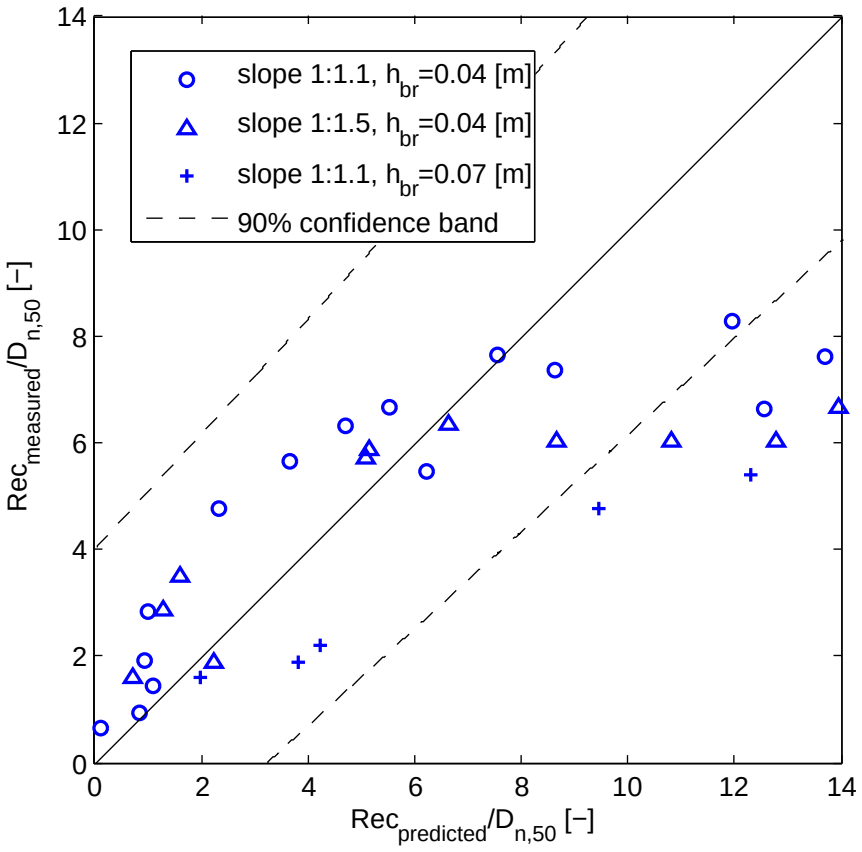

Figure 8.1. Validation of results.

These confidence intervals are established by Lykke Andersen [2006]. The author plots the 90% confidence bands both for the data used in the study, and for all the data available. The latter is used in the equations below. Equation (8.1) is for the upper limit, while the lower limit is set by Equation (8.2).

$$\frac{Rec_{95\%}}{D_{n,50}} = 1.080 \cdot \frac{Rec_{50\%}}{D_{n,50}} + 4.00 \tag{8.1}$$

$$\frac{Rec_{5\%}}{D_{n,50}} = 0.909 \cdot \frac{Rec_{50\%}}{D_{n,50}} - 2.95 \tag{8.2}$$

The predictions fit the measurements, with an overestimation especially in the cases of high measured recession. This overestimation is the subject of the subsequent sections of this report.

8.1.2 Recession using the Moghim method

This method for predicting berm recession has been described in Section 2.5. The present tests lie within the validity ranges of the formula, thus allowing comparison. This is done in Figure 8.2.

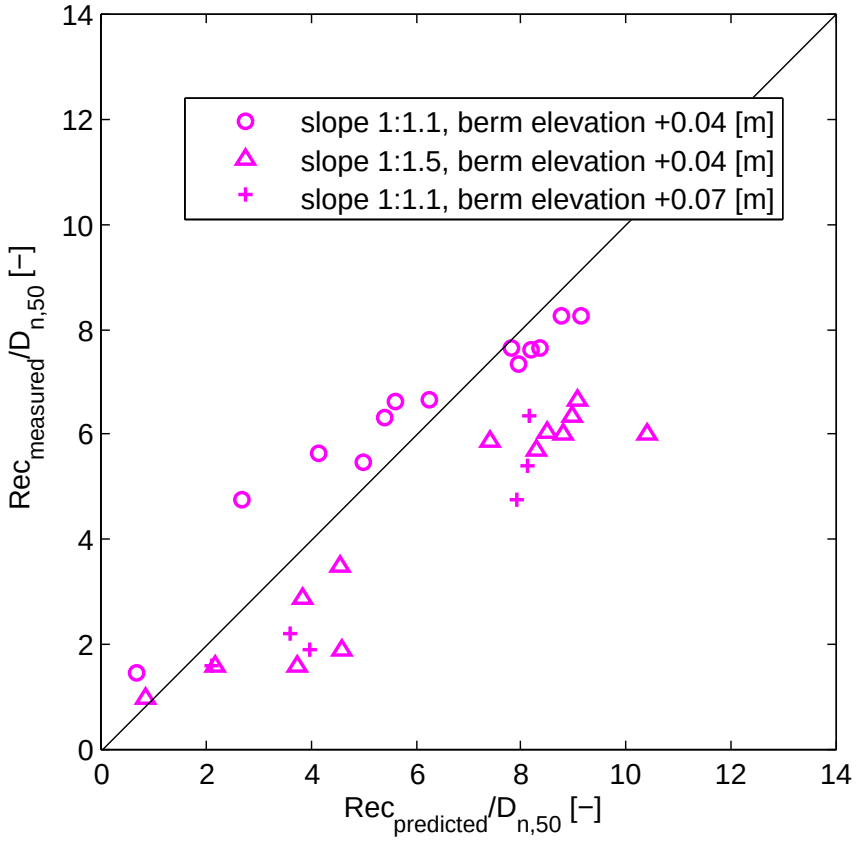

Figure 8.2. Evaluation of Moghim recession formula.

The method proves very successful in predicting recession in all the situations. From Figure 8.2, the following observatios can be made:

- The predictions are on the conservative side for all situations with a *high berm*. (+ shapes in Figure 8.2)
- In all but one case, the predicted recession is higher than the measured one for *low berm - flat slope* situations. (△ shapes in Figure 8.2)

Based on these first observations, it can be said that there is a noticeable separation between the three cases. The formula does not take into account the initial front slope, and is derived using tests done exclusivelly with a 1:1.25 front slope. The experiments conducted for the present study are limited to a 1:1.1 and 1:1.5 front slope, making it impossible to directly compare to the results of [Moghim et al., 2011]. It is clear from Figure 8.2 that a complete berm recession formula should include the influence of front slope.

The formula takes the effect of berm elevation into account by the factor h_{br}, as shown in Equation (8.3).

$$\frac{Rec}{D_{n,50}} = a_1 \left(\frac{h_{br}}{H_s} \right)^{-0.2} \tag{8.3}$$

Considering the separation of *low-berm* and *high-berm* results, the influence of berm height should be further investigated.

8.1.3 Recession estimation using the van der Meer method

Information about recession can be obtained using the method from van der Meer [1992]. As can be concluded from Chapter 2, this method of calculating recession is designed for dynamically stable slopes, with a parameter $H_s/\Delta D_{n,50}$ in the range 3- 500. van der Meer [1992] studies the lower part of this range, focusing on values smaller than 6. Nonetheless, the present tests lie outside the intended range of this formula.

An attempt was made to obtain information about berm recession for the present case using this formula. A reshaped profile is obtained through the use of a computer program. The top part of the reshaped profile, at its intersection with the berm elevation, determines recession. A detailed description about the application of the formula is found in Appendix B.2. The comparison between the current measurements and the predictions obtained from the formula are plotted in Figure 8.3. A comparison between the recession estimation methods will be made at a later stage in the report.

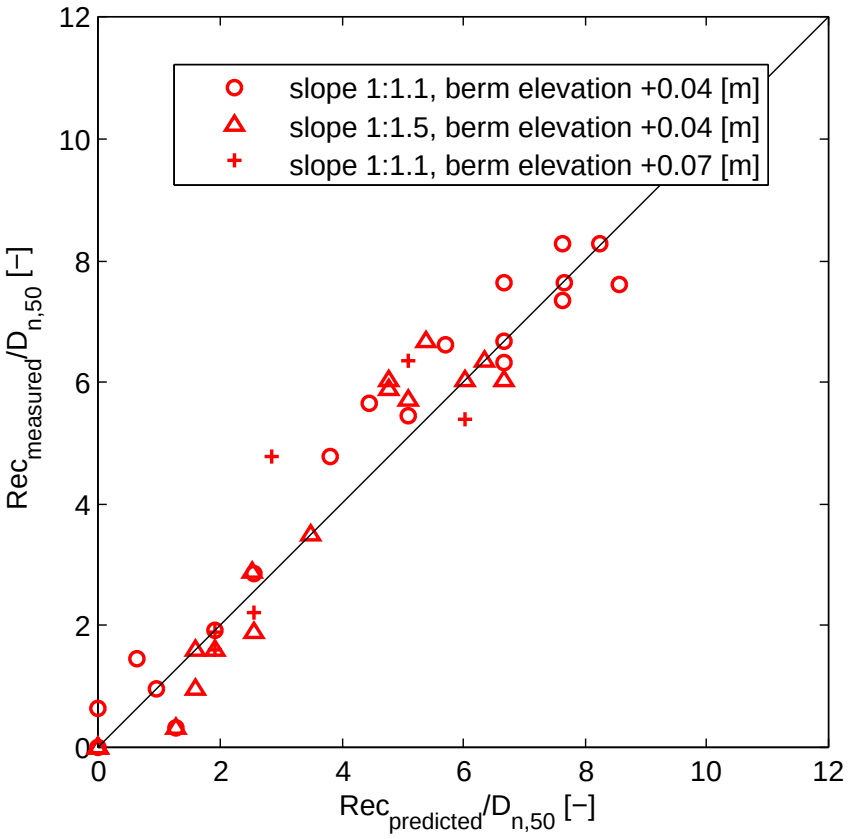

Figure 8.3. Validation using the van der Meer method.

The method estimates the recession quite well, even for the steeper slope that was initially outside the range tested by van der Meer [1988]. Also, the method predicts the recession for *high-berm* cases quite accurately. It is found that the method is successful in predicting berm recession in the range of H_0T_0 reached in the present experiments.

8.1.4 The Tørum formula

This method of calculating recession, proposed by Tørum and Krogh [2000], was described in Section 2.3. The formula takes into account just the stability parameter H_0T_0, and the stone gradation. Because of the limited number of parameters considered, the formula is difficult to analyze further. Figure 8.4 shows the comparison with the current data. In all cases the recession is underpredicted.

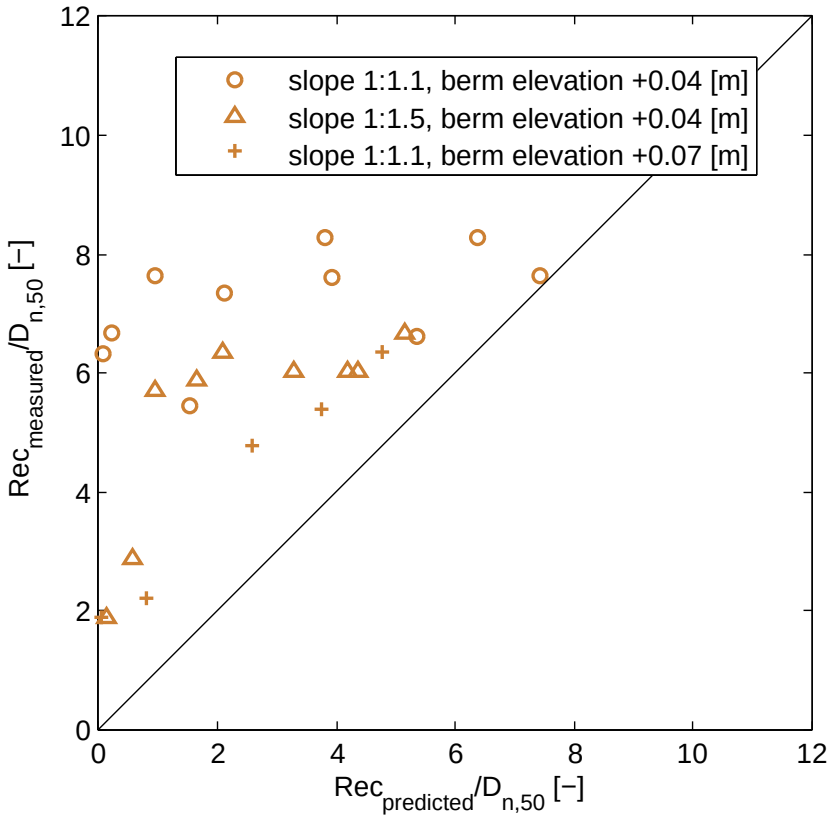

Figure 8.4. Comparison of measurements to the recession formula.

Missing several important parameters, this formula can be considered not reliable when compared to the other methods of estimating recession.

8.1.5 The Shekari method

From the papers considered in this report, Shekari and Shafieefar [2012] is the only one who considers the influence of berm width.

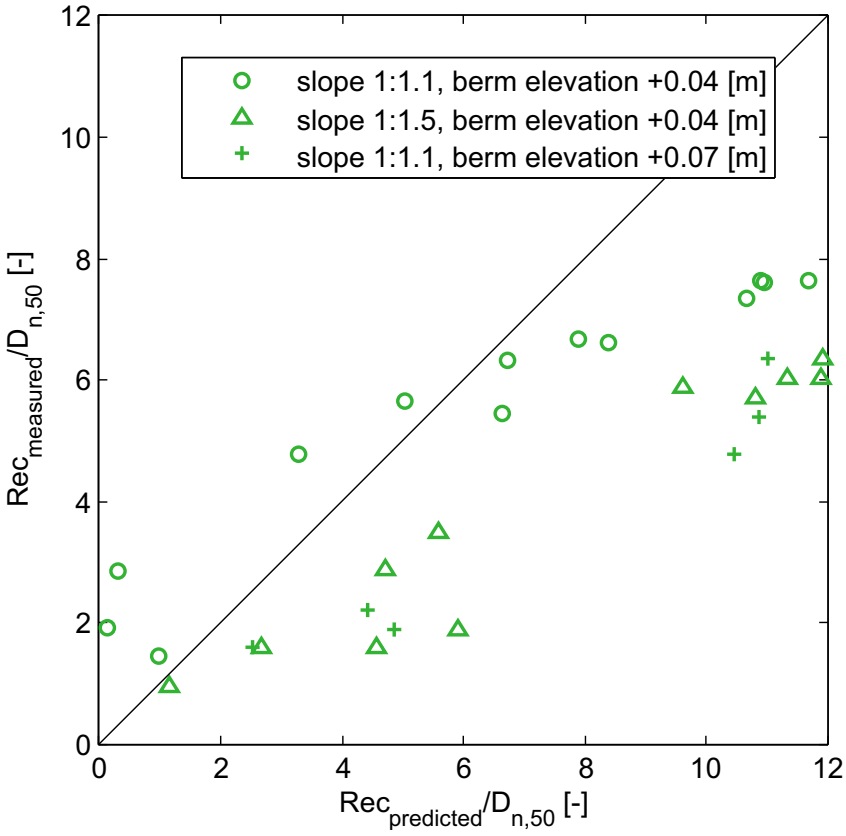

Figure 8.5. Comparison of present data with formula.

The formula is relatively simple and is based on the new stability parameter, $H_0\sqrt{T_0}$. The distinctive feature of this formula is the inclusion of the berm width in recession calculation. The berm width is not varied for the present data and is set to a constant $B = 0.25[m]$. Therefore it is not possible to evaluate the performance of the formula for different berm widths. However, when looking at Figure 8.5, it can be seen that there is a tendency to overestimate recession. When looking at the figure, it is not clear why the formula has the tendency to give such high results for some situations. No separation between the cases is obseved. The situations where very conservative results are seen are identified as the ones with a high wave height, H_s. The influence of H_s over calculated recession can be seen in Figure 8.6.

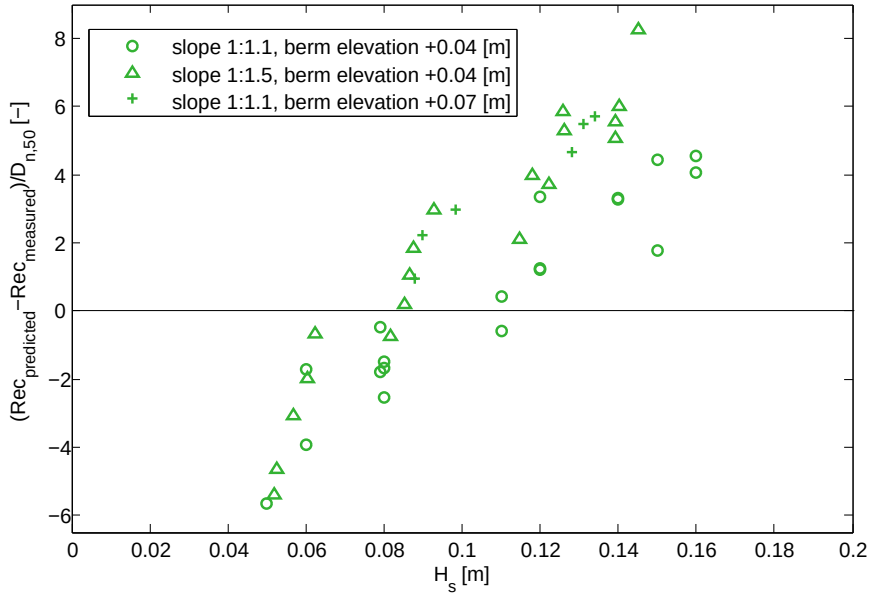

Figure 8.6. Evaluation of the influence of wave height.

In the formula, the wave height influence is included both by the parameter $H_0\sqrt{T_0}$, and in the parameter that includes the influence of the berm elevation, $(h_b/H_s)^{-0.21}$. By analyzing the magnitude of each factor, the cause of overestimation is identified as ultimately being the use of $H_0\sqrt{T_0}$, as illustrated in Figure 8.7. It is worth noting that some of the tests are outside the range intended for this formula, more specifically the ones with $H_0\sqrt{T_0} \leq 7.09$. Nevertheless theese tests were included in the figure and show similar behavior as the other ones.

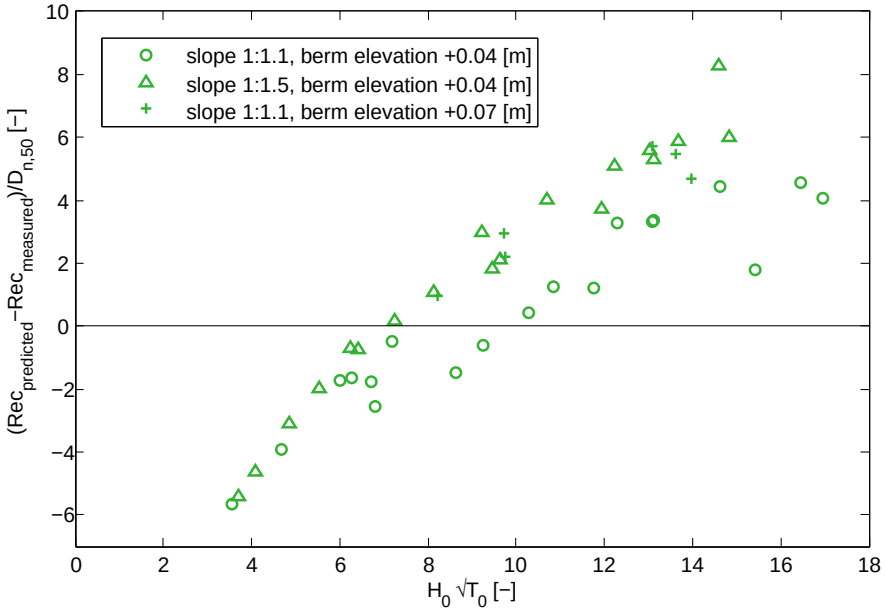

Figure 8.7. Evaluation of the influence of $H_0\sqrt{T_0}$.

Shekari and Shafieefar [2012] is a new formula, and has been tested by the authors using a large spectum of data from other researchers. It is possible that further refinement

might be necessary in the use of $H_0\sqrt{T_0}$. Because of the lack of berm width variation in the present data, it was not possibe to evaluate its efficiency in predicting recession for those situations. Introducing the berm width into the recession calculation could be an important addition to recession formulas.

8.2 Parameter influence evaluation

In this section, certain variables will be isolated from the formulas described in Section 2 and evaluated in Section 8.1 against the present data. All parameters are considered, but not all are investigated. The parameters studied in this section are selected by the following criteria:

(a) The parameter has an important effect in the formula, i.e., the formula is sensitive to the parameter.
(b) The parameter is deemed proeminent due to an observed phenomena, or suggestion by previous studies.
(c) The present data can be used in the investigation of the named parameter.

Naturally, a full investigation by looking at all the factors involved would yield a much more complex image. However, due to the limited time made available for this report, only the most relevant parameters were chosen to be investigated.

8.2.1 Skewness

The investigation of this parameter is related to the Lykke-Andersen formula, where skewness is considered in order to include the influence of breaking waves. An explanation for the overestimation of the recession can be the presence of breaking waves and the importance attributed to them in the formula. The Lykke-Andersen formulas uses the skewness factor f_{sk}, which is an exponential function of the square of the skewness, b_1. As a result, for cases of high non-linearity, the factor f_{sk} gives high values. This is confirmed by checking the magnitude of the skewness factor for the current data. It can be seen that it ranges between 1.07 and 2.30.

Lykke Andersen [2006] proposes a simple way of estimating the wave skewness, based on the Ursell number, that is shown in Equaiton (8.4). The Ursell number measures the importance of non-linearity, and values larger than 1 are considered indicative of high non-linearity.

$$Ur = \frac{H_{m0}}{2 \cdot h \cdot (k_p h)^2} \tag{8.4}$$

$$k_p = \frac{2 \cdot \pi}{L_p} \tag{8.5}$$

Where:

H_{m0}	significant wave height	$[m]$
h	water depth	$[m]$
k_p	peak wave number	$[-]$
L_p	peak wave length	$[m]$

After calculating the Ursell number, the wave skewness can be estimated by Equation (8.6).

$$b_1 = 0.54 \cdot Ur^{0.47} \tag{8.6}$$

In Figure 8.8, a comparison is made between the measured skewness of the waves and the predictions obtained using the method described above. The fit can be considered accurate.

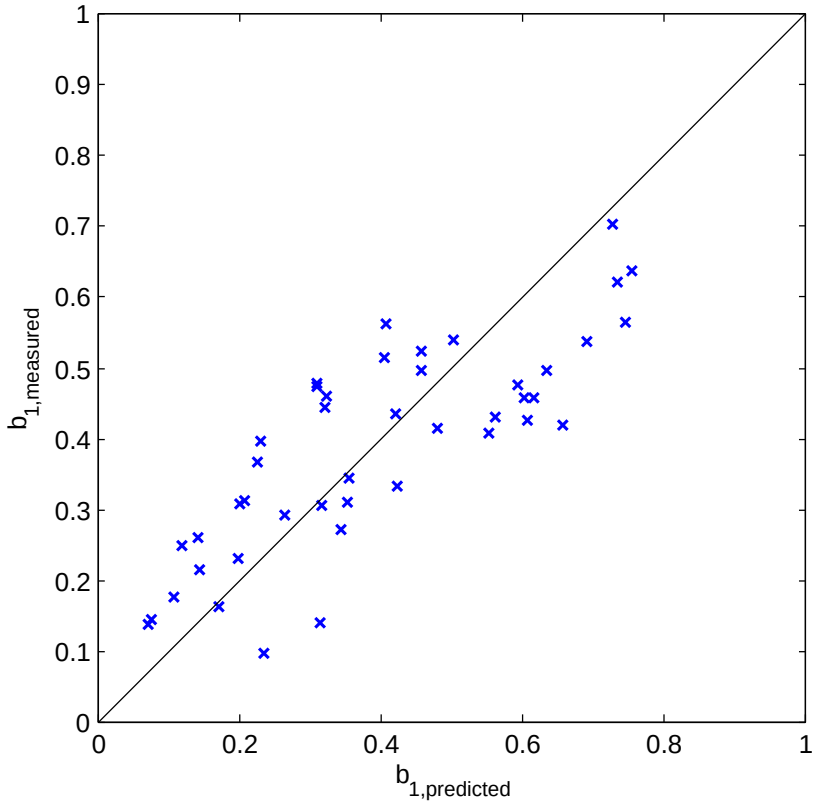

Figure 8.8. Skewness compared.

Equation (8.6) shows the relation considered between b_1 and the Ursell number. In Figure 8.9, the blue marks represent the present data, while the black curve represents the relationship between b_1 and Ur, as given by Equation (8.6). For the cases where the relative importance of non-linearity is large, the proposed relation provides conservative estimations in all cases. Overestimation increases with increasing non-linearity.

For the purpose of further investigation, the present data is fitted with a new distribution, obtaining a different formula for b_1, given in Equation (8.7).

$$b_1 = 0.481 \cdot Ur^{0.268} \tag{8.7}$$

Figure 8.9 shows the new fit, together with the present data and the original formula for skewness. The blue line, representing Equation (8.7), fits the data much closer than the black curve, representing Equation (8.6). Both are power fit functions of the type $y = a \cdot x^b$. Lykke Andersen [2006] obtains the correlation between the Ursell number and wave skewness largely based on thests with a value of Ur smaller than 1 (for the majority of data used, $Ur \leq 0.8$), which can explain the adequate fit up to and including $Ur = 1$, while giving overestimations in cases of higher Ursell numbers.

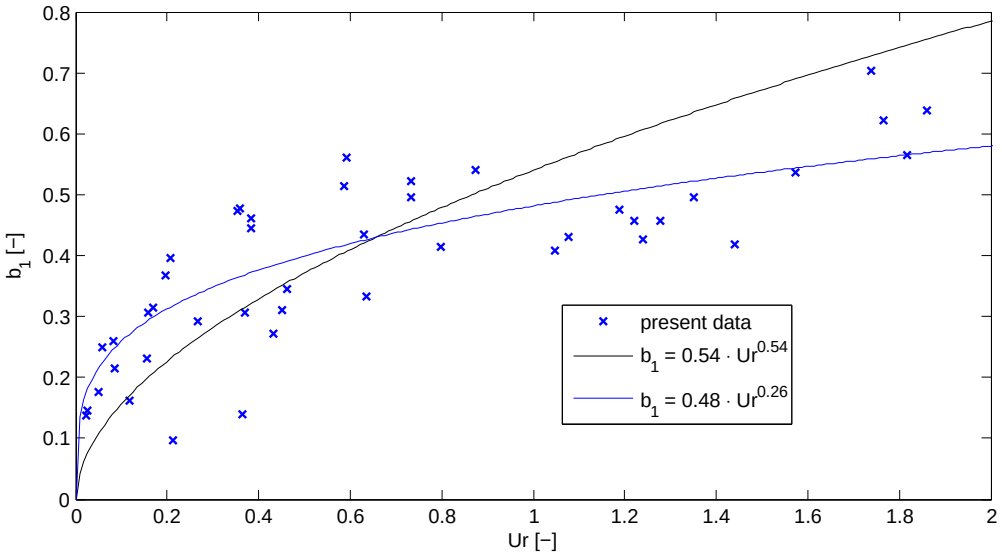

Figure 8.9. Alternative fit for b_1.

Extra analysis of this parameter is done by considering the influence of breaking waves unimportant, i.e., setting $b_1 = 0$ when performing the recession estimation with the Lykke-Andersen formula. When the influence of skewness is neglected, the Lykke-Andersen formula yields much more accurate results in this case. In Figure 8.10, the red symbols represent the data points for which the predicted recession is obtained by setting $b_1 = 0$. As it can be seen, all data poins fall within the confidence intervals.

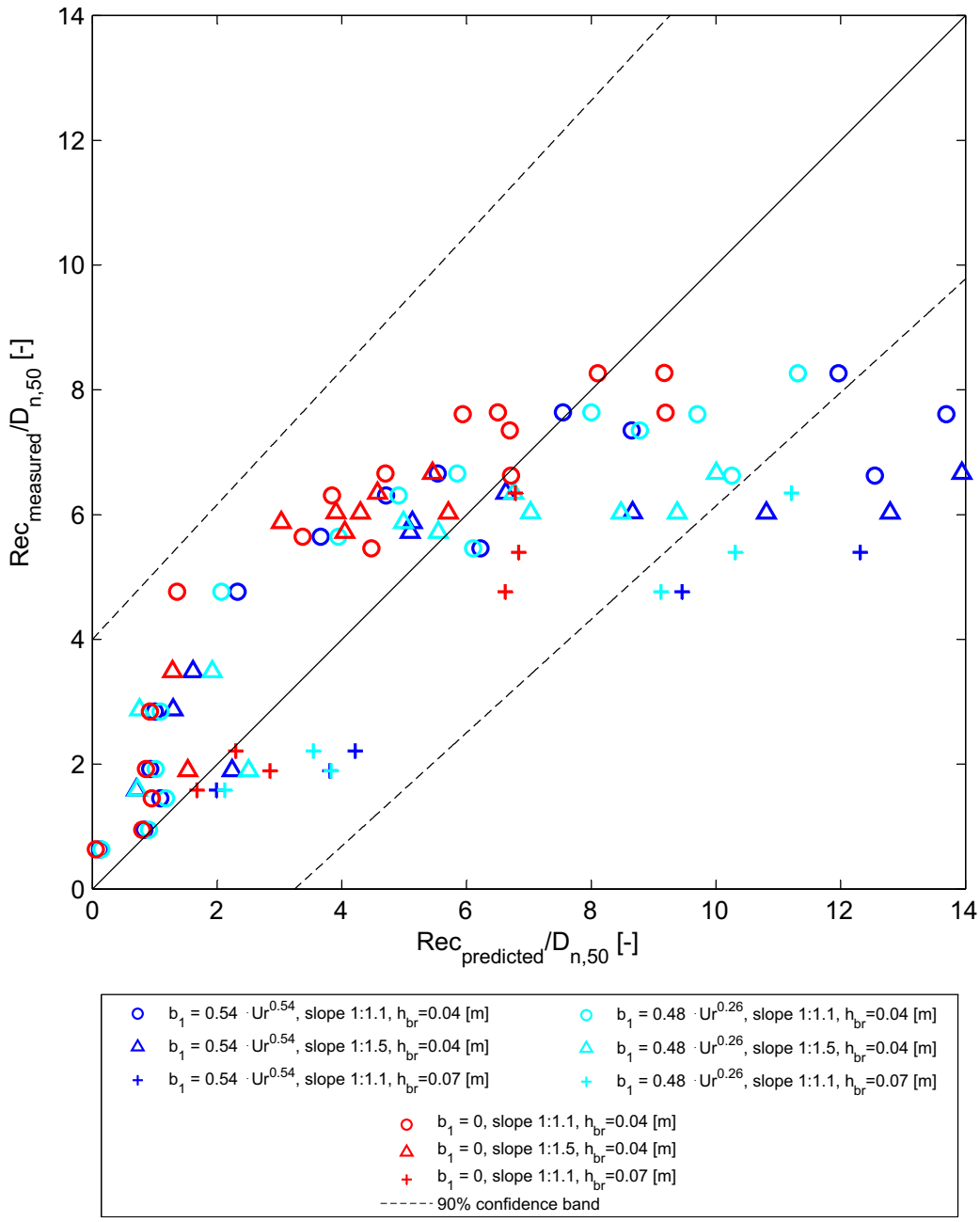

Figure 8.10. Skewness effect on predicted recession.

Considering the results of the present analysis, it can be concluded that, ultimately, when estimating recession using the Lykke-Andersen formula, the best results are obtained when neglecting the influence of b_1 entirely.

8.2.2 Step height

Another parameter in the Lykke-Andersen formulas is the step height h_s, defined as the distance from the SWL to the location where the slope becomes flatter than 1:2. The location of this point is illustrated in Figure 8.11.

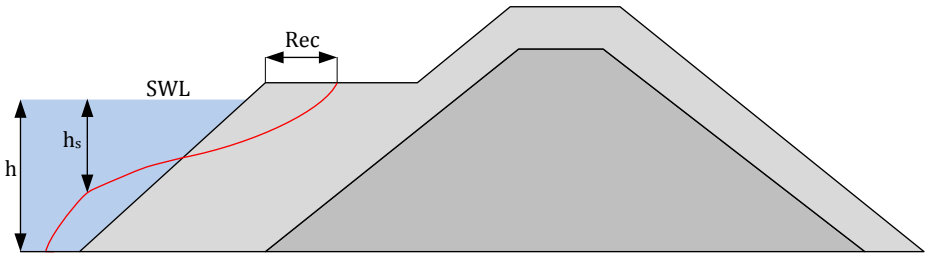

Figure 8.11. Location of the step height, h_s on a berm breakwater.

The formula for calculating the step height is given in Equation (8.8). This formula is obtained by curve fitting of the Lykke Andersen [2006] data.

$$h_s = 0.65 \cdot H_{m0} \cdot s_{0m}^{-0.3} \cdot f_N \cdot f_\beta \tag{8.8}$$

As it can be seen from the above equation, one assumption made for the derivation of the formula for h_s is that the step height is independent of the initial geometry. This assumption, along with the accuracy of the prediction of the step height can be tested against the current data.
A *MatLab* function was developed to identify h_s on the reshaped profiles from the present experiments. The function implements the definition given earlier by setting a threshold for the slope, as can be seen in Figure 8.12.

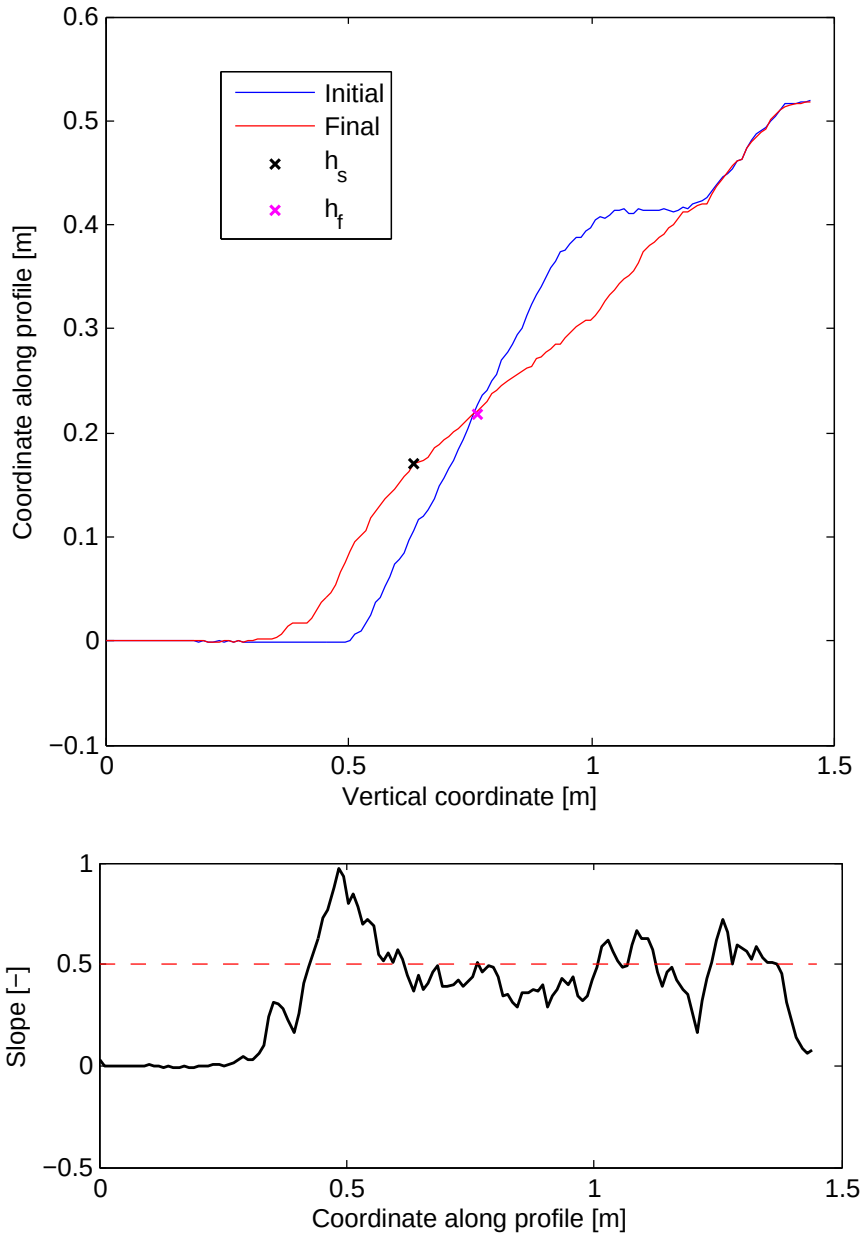

Figure 8.12. Identifying the step height and profile intersection, Test 613.

By employing this method, step heights for all the conducted tests are measured, with good reliability. This method has proved reliable when compared to visual measurements, however, it has also provided values for h_s in the rare case where a step height is not clearly visible. This is an attestation of the difficulty of defining a step height. Nonetheless the definition is followed and a comparison can be made. The comparison between measurements and calculations is made in Figure 8.13. The situations with very low damage, the ones that have an indistinguishable step, are omitted from the plot.

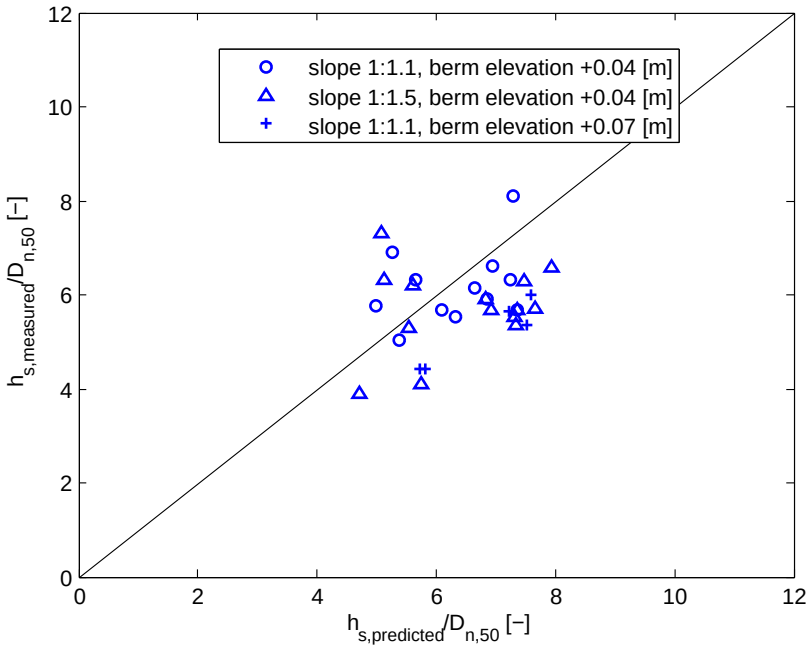

Figure 8.13. Evaluation of h_s.

As it can be seen, the assumption of h_s being independent on initial geometry is valid, and the formula provides a good agreement with the results. The method for predicting the step height gives good results regardless of the initial front slope and initial berm height. A small tendency is noticed concerning the variation of berm height. In the case presented in Figure 8.13, all *high-berm* tests have an overestimated h_s. An explanation for this may be that the independence on initial geometry may only be valid for certain h_{br}/h or H_{m0}/h ranges. It makes sense that in the case of a high berm, more material is available to be displaced from above SWL. This could lead to the creation of a step that is higher than for a *low-berm* structure, making h_s smaller. This phenomenon might occur in certain H_{m0}/h conditions, or h_s could be dependent on $k \cdot h$, where k is the wave number.
The influence of berm elevation was a secondary aspect of this project, and the limited number of tests performed in that regard doesn't provide a conclusive proof of overestimation. Consequently, the conclusions of van der Meer [1988] and Lykke Andersen [2006] are used, and the influence of berm height may be investigated further. This can be done by analyzing a larger collection of data containing tests with various berm heights and various water depth parameters. By doing this, certain limits of Equation (8.8) can be found, or other parameters can be included in the formula.

8.2.3 Stability parameters

The stability parameter H_0T_0 has been used as a governing parameter for recession for large H_0, and in the Lykke-Andersen formula the influence of T_0 is ignored in the cases of low H_0. The parameter used to introduce the effect of stability parameters in the Lykke-Andersen formula is f_{H_0}, defined in Equation (8.9). The second branch of the equation is considered valid for $H_0 > 5$, and the first branch for $H_0 < 3.5$. Equation

(8.10) is the transition point between the formulas. It can be seen that, even if T_0 is not included for the cases of low stability numbers, the wave period is still accounted for through s_{0m}.

$$f_{H_0} = \begin{cases} 19.8 \cdot \left(\frac{-7.08}{H_0}\right) \cdot s_{0m}^{-0.5} & for\ T_0 \geq T_0^* \\ 0.05 \cdot H_0 T_0 + 10.5 & for\ T_0 < T_0^* \end{cases} \tag{8.9}$$

$$T_0^* = \frac{19.8 \cdot exp\left(\frac{-7.08}{H_0}\right) \cdot s_{0m}^{-0.5} - 10.5}{0.05 \cdot H_0} \tag{8.10}$$

In this report, all the tests have a value of $H_0 < 2.89$, so the first branch of Equation (8.9) is followed, implying a small influence of the wave period. Figure 8.14 shows an evaluation of f_{H_0} with the present data. No tendency of variation is noticed. It should be noted that, in the plotting of Figure 8.14, the Lykke Anderson formula with the adjusted b_1 was used.

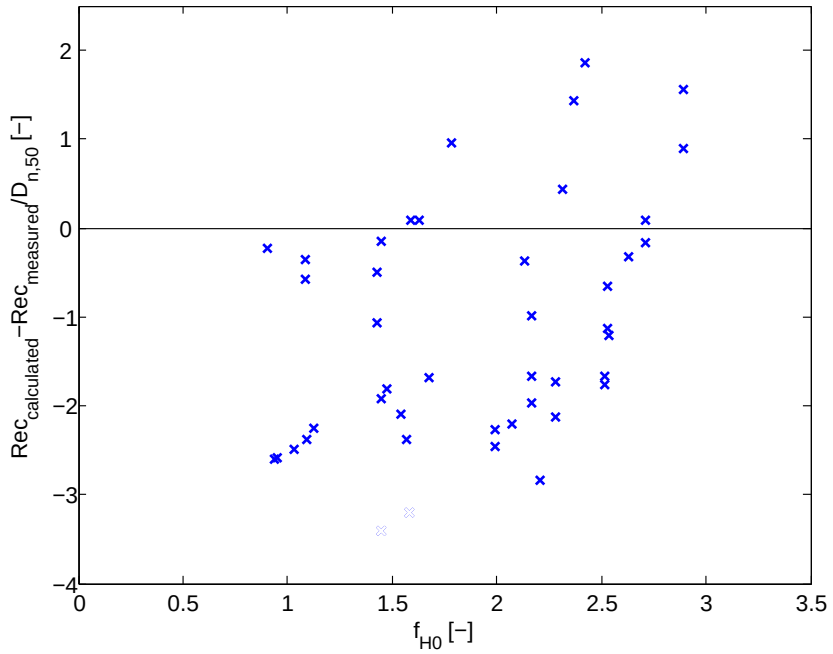

Figure 8.14. Evaluation using f_{H_0}.

It can be concluded that the influence of stability numbers is included in the Lykke-Andersen formula in a proper manner, and neglecting T_0 for low stability numbers is a valid consideration. As stability indexes of $H_0 > 5$ are of little concern when dealing with berm breakwaters, no tests have been included in that range. To cover the second branch of Equation (8.9), Lykke Andersen [2006] uses the data of van der Meer [1988], which covers dinamically stable situations, with higher values of H_0.

8.2.4 Influence of number of waves

The influence of number of waves has been assessed by performing a series of short-tests, consisting of approximately 250 irregular waves each. After each test, the breakwater profile was scanned and the next test was started. The difference between these tests and the ordinary ones is that the breakwater was not rebuilt after each test. By not rebuilding it, it is possible to observe how the stable profile is developing.
In Figure 8.15, the scanned profiles are plotted against each other. It can be seen that, although the numbers of waves are kept constant for all the tests, the difference in eroded area between two consecutive tests is decreasing. This is a sign that the breakwater profile has become more stable.

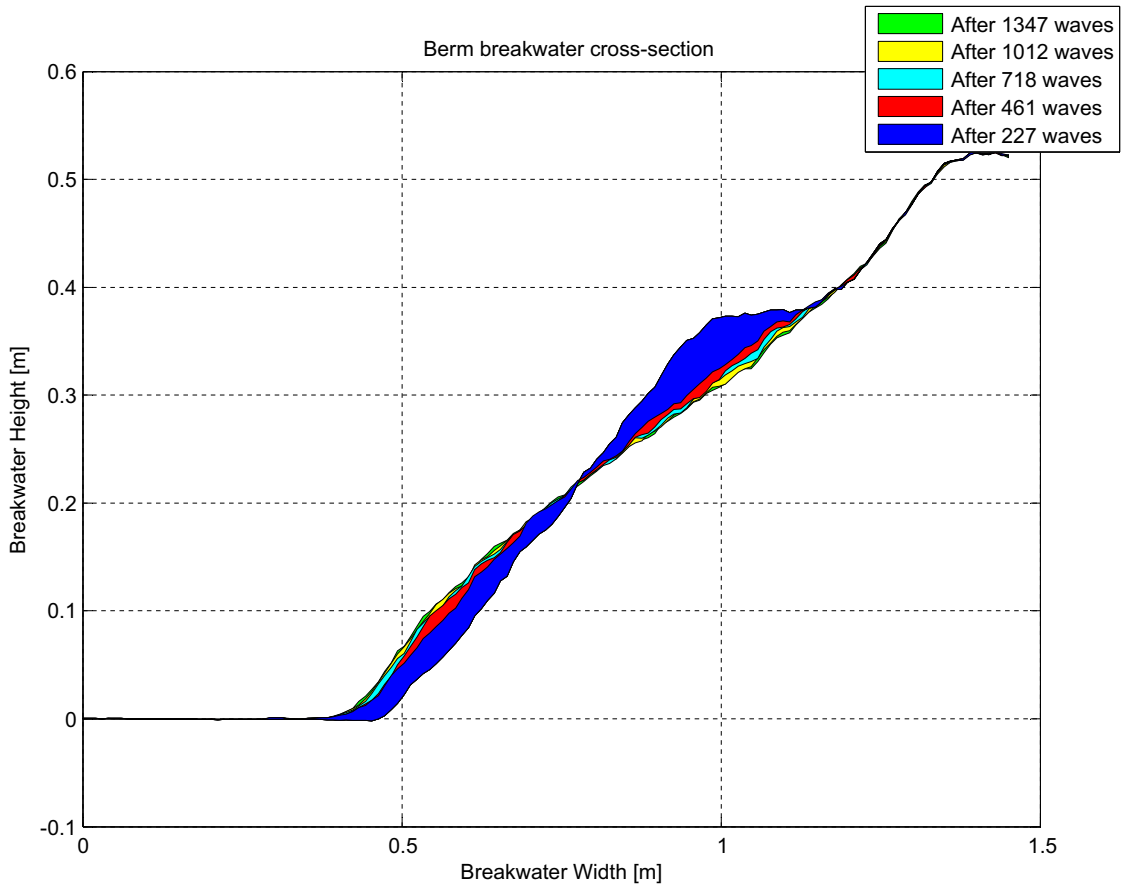

Figure 8.15. Influence of number of waves.

To get a better overview of this effect, Table 8.2 shows in numbers the eroded area for each test.

Table 8.2. Results from 'Influence of number of waves' tests.

Test Name	Eroded Area, Ae $[m^2]$	Number of waves per test, N $[-]$
300	$9.401 \cdot 10^{-3}$	227
301	$11.408 \cdot 10^{-3}$	234
302	$11.604 \cdot 10^{-3}$	257
303	$11.643 \cdot 10^{-3}$	294
304	$11.644 \cdot 10^{-3}$	335

It is obvious that after 1347 waves the breakwater reached a stable 'S' shape profile. After this point, if the tests were to continue there would be little or no damage no matter how long the tests were to last.
The influence on number of waves was studied before by van der Meer [1988], where a formula for estimating the total damage using the number of waves was developed, Equation (8.11).

$$S(N)/S(5000) = 1.3[1 - exp(-0.0003 \times N)] \tag{8.11}$$

Where:

S	Damage	$[-]$
N	Number of waves	$[-]$

As illustrated in Figure 8.16, if this formula is applied to the data the present project gained from the laboratory tests, the results are unreliable.

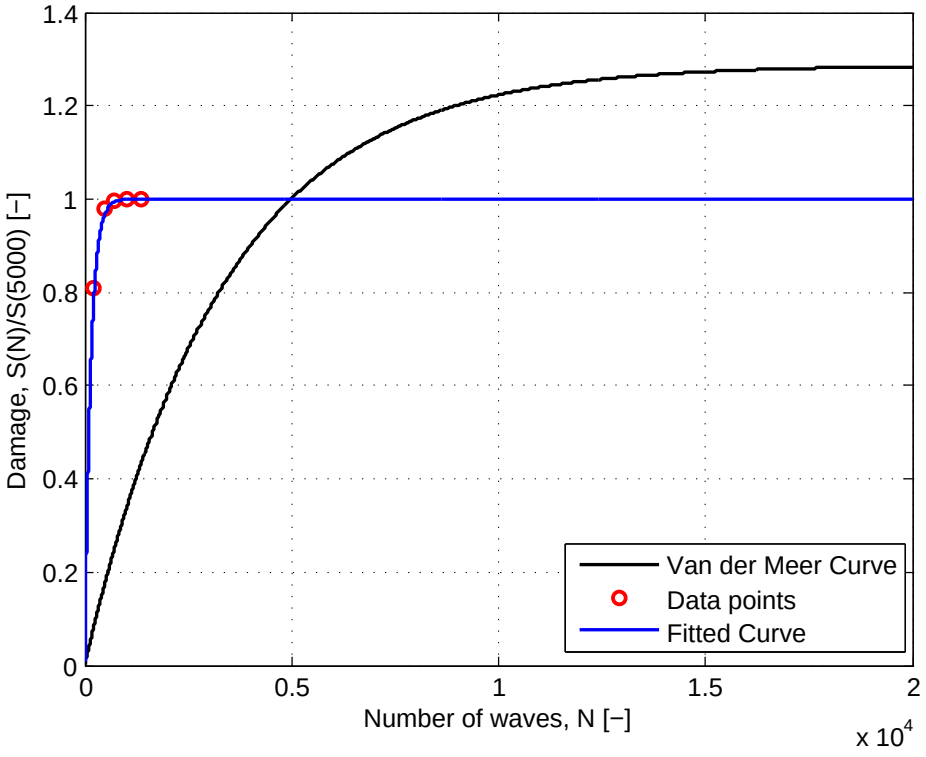

Figure 8.16. Influence of number of waves on damage.

This unreliability is due to the big difference in estimated and calculated damage when using Equation (8.11).
An explanation to this is that van der Meer [1988] used a conventional rubble mound breakwater, while the present project used a berm breakwater. As already discussed in article Lykke Andersen [2006], the damage of reshaping berm breakwaters will develop sooner than a for a conventional rubble mound breakwater due to smaller resistance to wave actions.
Another explanation is the front slope angle; the present project used $cot(\alpha)1.1$ while article van der Meer [1988] used much flatter front slopes, $cot(\alpha) > 1.5$. Clearly, a steeper slope will be more unstable, thus the damage will develop sooner.

8.3 Comparison between methods

In this section, the methods of calculating berm recession investigated in the previous sections are compared. The comparison is made using the adjusted formulas, as Section 8.2. Only the most promising methods of berm recession estimation - Lykke-Andersen, van der Meer, and Moghim - are plotted in Figure 8.17. A figure containing a full comparison is available in Appendix D. At the begining of this chapter, a symbol convention has been established to distinguish the different formulas and test configurations. The convention is repeated here, in Table 8.3, which is also designed to serve as a legend for Figure 8.17.

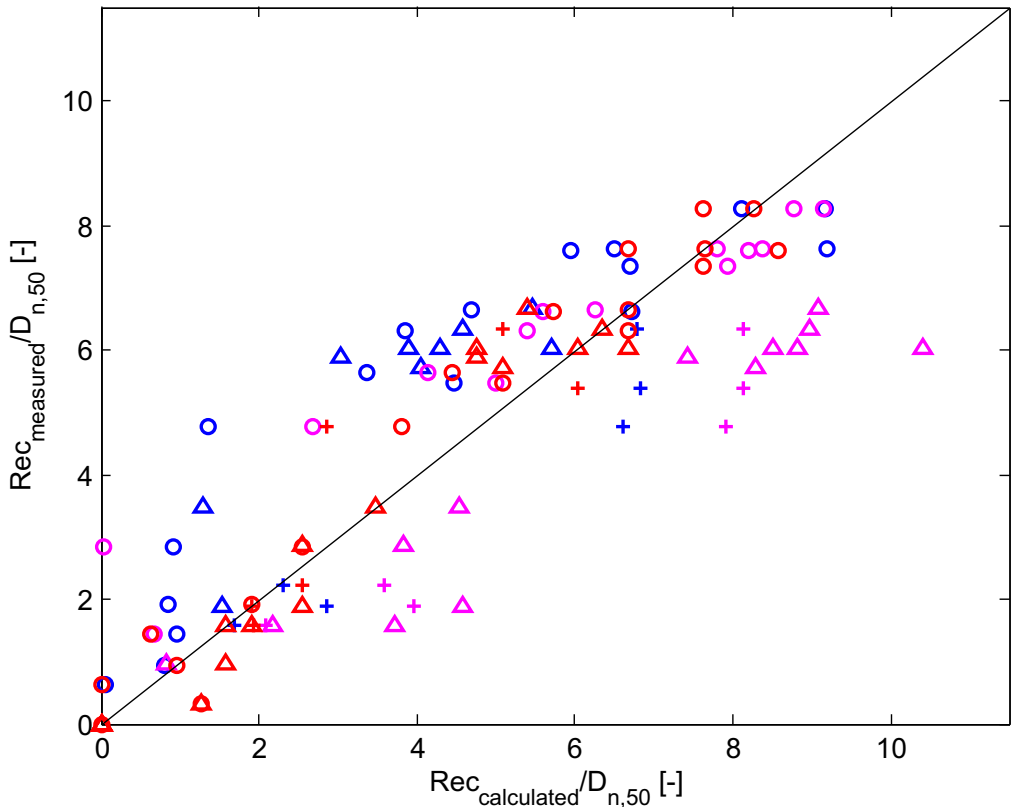

Figure 8.17. Comparison of the Lykke-Andersen, van der Meer, and Moghim results.

Table 8.3. Symbol convention for Figure 8.17.

Berm elevation:	$0.04[m]$	$0.04[m]$	$0.07[m]$
Front slope:	1:1.1	1:1.5	1:1.1
Lykke-Andersen	◯	△	+
Moghim	◯	△	+
van der Meer	◯	△	+

To evaluate the reliability of the formulas, a validation index is used. This is the coefficient of determination, R^2, which in this case is the square of the correlation coefficient. The values are shown in Table 8.4. A theoretical value of $R^2 = 1$ shows a perfect fit between the results and predictions.

Table 8.4. R^2 for different methods.

Method	$R^2[-]$
Lykke-Andersen	0.852
Moghim	0.788
van der Meer	0.943

The estimation potential for all three formulas can be considered very good. By applying the adjustments suggested in Section 8.2, the value of R^2 for the Lykke-Andersen formulas has been increased signifficantly. The van der Meer method shows the best results, but, due to the use outside its limits, further study is suggested. When evaluating the complexity of the recession estimation methods, the Lykke-Andersen is revealed as the most versatile formula. The need for a elaborate computer program to be used in conjunction with the van der Meer method deems the estimations more prone to errors, and makes it less suitable for basic, direct recession estimation. From a complexity point of view, the Moghim formula is the most rewarding, considering that it yields relatively reliable results given its simplicity.

9 Overtopping

Article Lykke Andersen [2006] proposed a new formula for estimating overtopping. The formula is illustrated in Equation (9.1); it is valid for breakwaters with no superstructures and gives the overtopping discharge at back of the crest.

$$Q_\star = 1.79 \cdot 10^{-5} \cdot (f_{H0}^{1.34} + 9.22) \cdot s_{0p}^{-2.52} exp[-5.63 \cdot R_\star^{0.92} - 0.61 \cdot G_\star^{1.39} - 0.55 \cdot h_{b\star}^{1.48} \cdot B_\star^{1.39}] \tag{9.1}$$

Where

$$Q_\star = \frac{q}{\sqrt{g \cdot H_{m0}^3}} \tag{9.2}$$

$$R_\star = \frac{R_c}{H_{m0}} \tag{9.3}$$

$$G_\star = \frac{G_c}{H_{m0}} \tag{9.4}$$

$$B_\star = \frac{B}{H_{m0}} \tag{9.5}$$

$$h_{b\star} = \begin{cases} \frac{3 \cdot H_{m0} - h_b}{3 \cdot H_{m0} + R_c} & for\ h_b < 3 \cdot H_{m0} \\ 0 & for\ h_b \leq 3 \cdot H_{m0} \end{cases} \tag{9.6}$$

$$T_0 = \sqrt{\frac{g}{D_{n,50}}} \cdot T_{0,1} \tag{9.7}$$

$$T_0^* = \frac{19.8 \cdot exp(-\frac{7.08}{H_0}) \cdot s_{0m}^{-0.5} - 10.5}{0.05 \cdot H_o} \tag{9.8}$$

$$H_0 = \frac{H_{m0}}{\Delta \cdot D_{n,50}} \tag{9.9}$$

$$f_{H0} = \begin{cases} 19.8 \cdot exp(-\frac{-7.08}{H_0}) \cdot s_{0m}^{-0.5} & for\ T_0 \geq T_{0\star} \\ 0.05 \cdot H_0 T_0 + 10.5 & for\ T_0 < T_0^\star \end{cases} \tag{9.10}$$

Where:

q	average overtopping discharge per meter structure width	$[m^3/m/s]$
$Q_\star$	dimensionless mean overtopping discharge	[-]
f_{h0}	factor accounting for the influence of stability numbers	[-]
s_{0p}	deep water peak wave steepness	[-]
$R_\star$	dimensionless crest freeboard	[-]
$G_\star$	dimensionless armor crest width	[-]
$h_{b\star}$	dimensionless berm elevation	[-]
$B_\star$	dimensionless berm width	[-]
R_c	crest freeboard	[m]
H_{m0}	significant wave height based on frequency domain analysis	[m]
B	berm width	[m]
h_b	water depth above berm	[m]
T_0	dimensionless wave period	[-]
T_0^*	dimensionless wave period transition point	[-]
H_0T_0	stability number including mean wave period	[-]
s_{0m}	deep water mean wave steepness	[-]

It is expected that, as the berm breakwater's front slope is being reshaped, the overtopping will be affected. This formula does not take into account the reshaping geometry of the breakwater as it does not contain any geometrical parameters, instead f_{h0} is used as an indicative measure of the reshaping.

Although this formula is based on tests with a front slope of 1:1.25 and in the present project front slopes varying from 1:1.1 up to 1:1.5 were used, the results fit very well. This is illustrated below, in Figure 9.1.

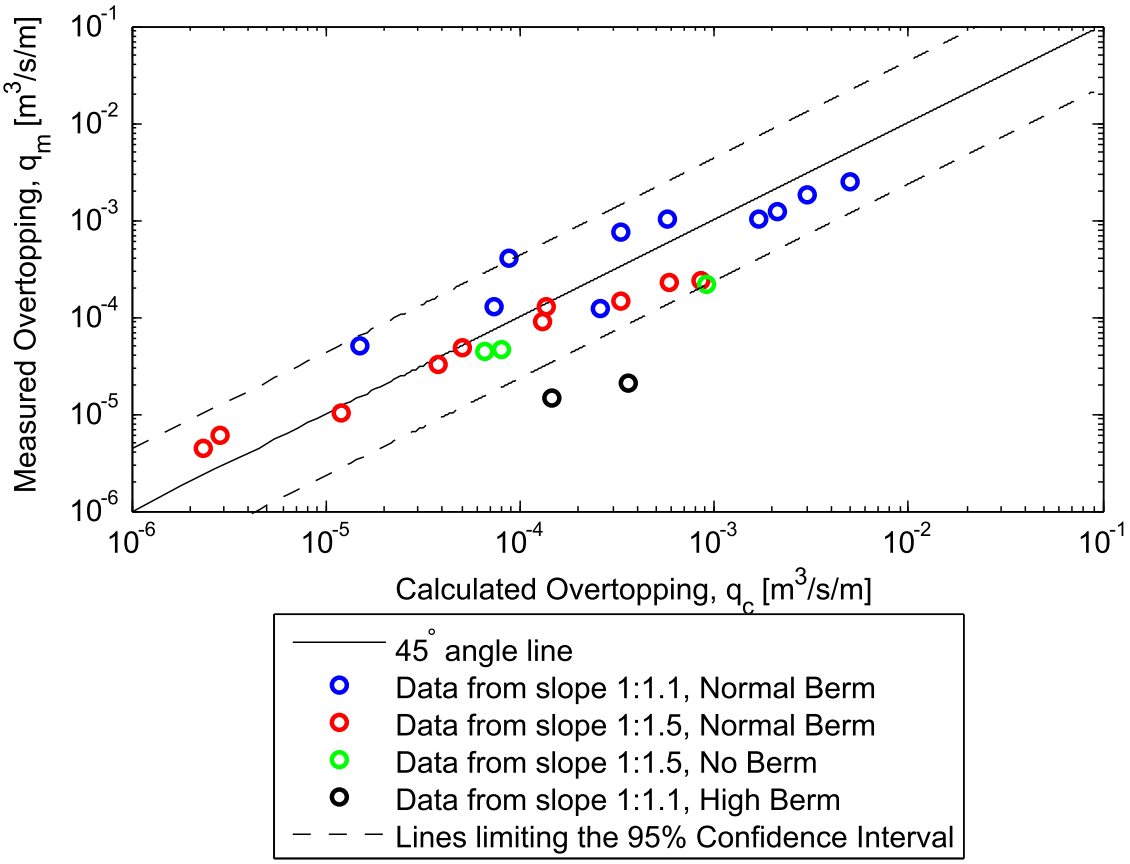

Figure 9.1. Overtopping Comparison.

Table 9.1 displays the results for overtopping, along with other results.

Table 9.1. Tests Results

Test Name	Hm0	Tp	Tm	T01	Number of waves	Skewness	H0T0	Recession	Eroded Area	Overtopping
111	0.07912	1.698	1.398	1.441	2567	0.2928	36.2577	4.6	0.003	0
112	0.1258	2.048	1.658	1.674	627	0.5231	66.9709	17.3	0.0181	0.0001043
113	0.1538	2.487	1.81	1.848	112	0.4959	90.3875	21	0.016	0.000458729
114	0.1618	2.901	1.969	1.955	364	0.5652	100.5948	24.2	0.0189	0.000636029
121	0.793	1.466	1.245	1.266	2865	0.2302	31.9269	6.1	0.0035	0
122	0.1148	1.832	1.511	1.524	2376	0.3444	55.6387	20	0.0142	1.54763E-05
123	0.1573	2.048	1.686	1.655	1246	0.5403	82.7898	26.21	0.022	0.000238574
124	0.1503	2.321	1.846	1.847	635	0.4193	88.2828	26.22	0.0226	0.000324344
131	0.06571	1.211	1.046	1.064	3395	0.2487	22.2343	1.01	0	0
132	0.0874	1.466	1.247	1.269	2890	0.3072	35.2714	9.02	0.005	0
133	0.1229	1.678	1.426	1.429	2453	0.4603	55.8514	21.11	0.0193	5.37082E-05
134	0.1414	1.896	1.531	1.526	1404	0.515	68.6205	23.3	0.0244	0.000170213
141	0.05235	0.941	0.8737	0.8842	4124	0.1381	14.7203	0	0	0
142	0.08597	1.17	1.062	1.071	3393	0.2594	29.281	3	0.0029	0
143	0.1146	1.365	1.245	1.237	2883	0.3671	45.0821	17.9	0.0128	6.23312E-06
144	0.1453	1.583	1.356	1.343	2647	0.4729	62.0571	24.21	0.0204	2.14755E-05
151	0.06404	1.989	1.686	1.743	2129	0.2721	35.4976	2.01	0	0
152	0.08717	2.579	2	2.022	1794	0.4081	56.0529	15.1	0.0113	0
153	0.1223	2.901	2.072	2.088	1732	0.6224	81.2096	24.12	0.0184	0.000134705
211	0.06253	1.719	1.401	1.457	2571	0.09688	28.9733	0	0	0
212	0.09622	2.079	1.67	1.719	2149	0.3328	52.6007	0.0042	0.0042	0
213	0.1298	2.321	1.86	1.873	1930	0.4578	77.3148	0.0123	0.0123	8.95578E-05
214	0.148	2.579	1.954	1.944	1189	0.5366	91.4973	0.0157	0.0157	0.000233419
221	0.05846	1.393	1.239	1.272	2459	0.1628	23.6481	0	0	0
222	0.08917	1.809	1.504	1.526	2387	0.3064	43.2736	0.0031	0.0031	0
223	0.1278	2.018	1.657	1.662	2166	0.496	67.5479	0.0144	0.0144	4.71764E-05
224	0.1522	2.321	1.749	1.753	2052	0.4312	84.849	0.0187	0.0187	0.000223935
231	0.05393	1.147	1.032	1.052	3474	0.1753	18.0425	0	0	0
232	0.08714	1.393	1.237	1.264	2897	0.3136	35.028	0.0028	0.0028	0
233	0.1221	1.707	1.409	1.425	914	0.4445	55.3326	0.0064	0.0064	1.01149E-05
234	0.1478	1.87	1.551	1.526	2308	0.5615	71.7264	0.0178	0.0178	0.000126324
241	0.05281	0.9548	0.8822	0.8915	4080	0.1452	14.9723	0	0	0
242	0.08362	1.208	1.073	1.077	3339	0.215	28.6402	0.0017	0.0017	0
243	0.1183	1.393	1.237	1.23	2305	0.396	46.2743	0.0045	0.0045	6.08422E-06
244	0.1451	1.534	1.363	1.345	2630	0.4775	62.064	0.0107	0.0107	3.29359E-05
251	0.0642	1.979	1.705	1.743	2102	0.3096	35.5863	0	0	0
252	0.09051	2.482	2.003	2.039	1788	0.4761	58.69	0.000489	0.000489	4.47117E-06
253	0.1262	2.905	2.086	2.047	1718	0.7035	82.1537	0.0145	0.0145	0.00014646
511	0.06519	1.625	1.268	1.427	2845	0.01859	29.5839	0	0	0
512	0.1004	2.008	1.469	1.698	2438	0.2	54.2153	0.0038	0.0038	0
513	0.1306	2.276	1.65	1.956	2172	0.2621	81.2386	0.0153	0.0153	4.66804E-05
514	0.155	2.528	1.959	2.261	1580	0.4848	111.4506	0.02288	0.02288	0.000214989
522	0.0904	1.728	1.487	1.646	2340	0.2384	47.3204	0.0052	0.0052	0
523	0.1331	2.101	1.621	1.842	2210	0.4867	77.9683	0.0167	0.0167	4.32755E-05
612	0.0985	2.038	1.648	1.842	2174	0.4352	52.9387	6	0.0087	0
613	0.131	2.354	1.859	2.115	1928	0.4578	78.1962	17.1	0.0224	0.000014708
622	0.08871	1.773	1.463	1.644	2450	0.14	42.7683	5.03	0.0049	0
623	0.1348	2.069	1.625	1.839	2173	0.4147	71.162	15.1	0.0089	0
652	0.09036	2.528	2.049	2.259	1499	0.4261	58.7939	7.01	0.006	0
653	0.128	2.905	2.106	2.391	1701	0.638	84.4246	20.11	0.0202	2.09241E-05

10 Conclusion

The aim of this project was to evaluate the berm recession formula and investigate some key parameters of these formulas. Some gaps in the knowledge about the reshaping and berm recession have been studied, for example by introducing the flatter slope, 1:1.5 in the investigation. In the current chapter, the findings of this report are described and some conclusions are drawn.

Firstly, some basic berm breakwater concepts have been investigated. Then, the current berm recession estimation methods have been investigated, bringing in to light the need for the current research. Based on this problem analysis, an experiment was devised. After the successful completion of laboratory tests, the data was processed and analyzed. The considered berm recession formulas have been tested against the current data. Finally, in a discussion chapter, the effectiveness of the formulas was studied and some improvements have been suggested.
The following berm recession estimation methods have been included in the current investigation:

- The Lykke-Andersen formula [Lykke Andersen and Burcharth, 2009];
- The Moghim method [Moghim et al., 2011];
- The van der Meer method [van der Meer, 1992];
- The Tørum formula [Tørum and Krogh, 2000];
- The Shekari method [Shekari and Shafieefar, 2012];

As first conclusion of this report, it can be said that the Lykke-Andersen formula, the Moghim method and the van der Meer method can be considered the most reliable formulas. As a general comment, it is seen that more complex formulas give better results. This statement is backed by the discussion in section 8.3, where the three methods mentioned above are compared directly using the present data. The Tørum formula, and the Shekari method both fail to provide appropriate estimations. The two formulas do not include some parameters that are considered very important, such as front slope, which may be the explanation for unsuccessful predictions.

The van der Meer method, that was applied outside its designed range, uses a complex computer program to predict the reshaping of the front slope. This method also gives very promising results when applied to the current data. Based on the equations from van der Meer [1992], the top part of the reshaped profile was predicted and recession was determined using the intersection of the initial profile and the calculated reshaped profile. Some problems might occur when using the *MatLab* code created for this project when calculating step height or volume conservation. Because *BREAKWAT* was not made available for this project, there were no means of comparison to the original computer program. van der Meer [1992] attests to the capabilities of *BREAKWAT* in computing the damaged profile for statically stable structures.

Although the *MatLab* code designed for this report predicts recession quite well, caution is advised in its use until further studies are made. The recession estimation is still based on the intersection between the original profile and the top part of the calculated reshaped profile, and not by means of erroded area. Moreover, the decision to include only the top part of the reshaped profile was made due to some problems encountered

when calculating the step height, and, sometimes, the step length. This decision proved valid if the precision of recession estimation is considered, however more investigation is required.

A possibility of obtaining the recession from eroded area could be to apply the Equation 10.1 [Lykke Andersen et al., 2012], where A_e is the eroded area, *Rec* is the recession, h_f is the depth of intersection between the original and reshaped profile, and h_b is the berm elevation.

$$A_e = 0.65 \cdot Rec \cdot (h_f - h_b) \tag{10.1}$$

The Lykke-Andersen formula can be considered the most "universal" of the berm recession estimation methods, as it includes the most parameters, and has the widest ranges tested. Additionally, the number of tests used to derive this formula is relatively large. The Lykke-Andersen formula has been studied closely in this report, and its parameters have been investigated. Most notably, the influence of breaking waves, accounted for in the formula by f_{sk}, was looked at. It has been suggested that the inclusion of influence of skewness might have been unnecessary in the ranges considered for berm breakwaters. By including skewness, the formula overestimates the recession for some tests where a high value of f_{sk} was obtained. A new formula for skewness was proposed, which assignes less importance to very non-linear cases. This formula was found to fit better with the present data, making the formula more precise. However, as it was concluded, the skewness can be neglected when using the Lykke-Andersen formula. The best fit with the current data was obtained when setting f_{sk} to zero.

The third best fit for the current data was obtained with Moghim et al. [2011]. This formula is one of the simpler ones, not including the influence of front slope. The formula si reasonably effective, however, the results clearly show that the influence of the front slope is not to be ignored. Also, the berm height, included in the formula by h_{br}/H_s, might have a smaller influence on recession than estimated using the Moghim formula. In all cases the method gives conservative estimates for *high-berm* cases. Considering the effectiveness of the formula, further study is encouraged, with the suggestion of including the influence of front slope.

Another suggestion for future improvement of berm recession formulas can be the inclusion of berm width. This is done by Shekari and Shafieefar [2012], who found that recession decreases with increasing berm width. With the data available for the present study, it was impossible to verify Shekari's findings. However, due to the interesting findings of this relatively recent study, further investigations should be made, especially considering the possible implications on the costs of a berm breakwater.

The study of the creation of a step on the reshaped profile, at depth h_s, has yielded some interesting results concerning mainly the separation of the *low-berm* and *high-berm* cases. Further refinement of the formula is suggested, by performing tests with different berm heights and water depth parameters. The *Matlab* code designed to identify h_s and h_f proved reliable.

The stability parameter $H_0\sqrt{T_0}$, introduced by [Moghim et al., 2011], takes in to account the influence of wave height and period on the stability, while reducing the importance

of T_0 compared to the stability parameter H_0T_0 used in previous studies. Keeping in mind the stability ranges for berm breakwaters, and especially the range with which f_{H0} is calculated in the Lykke-Andersen formula, it can be said that the inclusion of T_0 in the calculation might be unnecessary, as the wave period has little influence on reshaping. In the Lykke-Andersen formula, the wave period is accounted for by $s_{0m}^{-0.5}$. $H_0\sqrt{T_0}$ might warrant further investigation considering its potential, as highlighted by [Moghim et al., 2011].

As found in the paper by Lykke Andersen et al. [2012], the current study also confirms that the presence of the berm greatly influences the damage on the stucture when compared to straight slopes, as investigated by van der Meer [1988]. The seaward slope of the breakwater suffers more damage as waves become less steep, with no transition point detected between *surging* and *plunging* regimes. The van der Meer formulas for plunging waves are confirmed to predict stability even when used in the surging regime.

Referencing again to van der Meer [1988], it can be seen that the influence of permeability is neglected in subsequent studies. It has been proven that permeability has a significant effect on the stability of berm breakwaters. Permeability is a factor when dealing with the transmission of waves and overtopping, and might have an influence on recession. If the range of permeability for berm breakwaters is considered, it can be said that it is safe to assume that the variation permeability is not a great concern. However, it could be interesting to study several berm breakwater models with different permeabilities. The lower range of permeability is defined by a structure with an impermeable core, with P=0.1, while P=0.6 is an upper bound, which coincides with a homogenous structure.

Due to the limited time available for the realization of the current research, only the data generated by the current experiments has been used to reach the conclusions in this chapter. The researchers behind this project would suggest further refinement of this investigation by including data available from other researchers.

Part IV

Litterature

Bibliography

John Grønbech, Thomas Jensen, and Henning Andersen, 1996. John Grønbech, Thomas Jensen, and Henning Andersen. Reflection Analysis with Separation of Cross Modes. In *Proceedings of 25th Conference on Coastal Engineering*, 1996.

Hall, 1991. K.R. Hall. *Hydraulic model test results - A Study of the Stability of Berm Breakwaters.* Coastal Engineering, 1991.

Kao and Hall, 1990. J.S. Kao and K.R. Hall. *Trends in stability of Dynamically Stable Breakwaters.* Coastal Engineering, 1990.

Thomas Lykke Andersen. Hydraulic Response of Rubble Mound Breakwaters. PhD thesis, Aalborg Universitet, 2006.

Lykke Andersen and Burcharth, 2009. Thomas Lykke Andersen and H.F. Burcharth. *A new formula for front slope recession of berm breakwaters*. Coastal Engineering, 2009.

Thomas Lykke Andersen, J.W. van der Meer, H.F. Burcharth, and S. Sigurdarson, 2012. Thomas Lykke Andersen, J.W. van der Meer, H.F. Burcharth, and S. Sigurdarson. Stability of hardly reshaping breakwaters. In *33rd International Conference on Coastal Engineering*, 2012.

E.P.D Mansard and E.R. Funke. The Measurement of Incident and Reflected Spectra Using a Least Squares Method. In *Physical Models and Laboratory Techniques in Coastal Engineering*. World Scientific Publishing Co. Pte. Ltd, 1980.

Meinert, april 2006. Palle Meinert. *EPro user manual.* Aalborg University, 2006. Hydraulics and Coastal Engineering No.39.

Moghim, Shafieefar, Tørum, and Chegini, 2011. M.N. Moghim, M. Shafieefar, A. Tørum, and V Chegini. *A new formula for the sea state and structural parameters influencing the stability of homogenous reshaping berm breakwaters.* Coastal Engineering, 2011.

PIANC, 2003. PIANC. *State-of-the-art of designing and constructing berm breakwaters*, 2003.

Shekari and Shafieefar, 2012. Mohamed Reza Shekari and Mehdi Shafieefar. *An experimental study on the reshaping of berm breakwaters under irregular wave attacks.* Applied Ocean Research, 2012.

S. Sigurdarson, A. Jakobsen, O. Samarson, S. Bjørndal, C. Urrang, and A. Tørum, 2003. S. Sigurdarson, A. Jakobsen, O. Samarson, S. Bjørndal, C. Urrang, and A. Tørum. Sirevåg berm breakwater. Design, construction and experience after design storm. In *Proceedings of the International Conference on Coastal Strucutres*, pages 26–30, 2003.

Sigurdarson, Smarason, Voggosson, and Bjørdal, 2006. Sigurdur Sigurdarson, Omar Bjarki Smarason, Gisli Voggosson, and Sverre Bjørdal. *Wave height limits for the statically stable icelandic-type berm breakwater*. ICCE, 2006.

Tørum, 1998. A. Tørum. *On the stability of berm breakwaters in shallow and deep water.* Coastal Engineering, 1998.

Tørum and Krogh, **2000**. A. Tørum and S.R Krogh. *Berm Breakwaters. Stone Quality.* Civil and Enviromental Engineering, 2000.

Tørum, Moghim, Westeng, Hidayati, and Arntsen, **2011**. Alf Tørum, Mohammad Navid Moghim, Kenneth Westeng, Nurin Hidayati, and Øivind Arntsen. *On berm breakwaters: Recession, crown wall wave forces, reliability.* Coastal Engineering, 2011.

Jentsje van der Meer. Stability of seaward slope of berm breakwaters. PhD thesis, Delft Hydraulics, 1992.

Jentsje van der Meer. Rock Slopes and Gravel Beaches under Wave Attack. PhD thesis, Technische Universiteit Delft, 1988.

J.A. Zelt and J.E. Skjelbreia, *1992*. J.A. Zelt and J.E. Skjelbreia. Estimating Incident and Reflected Wave Fields Using an Arbitrary Number of Wave Gauges. In *Proceedings of 23rd Conference on Coastal Engineering*, 1992.

Part V

Appendix

A On berm breakwaters

A.1 Wave Run-up and Run-down

Run-up, R_u and run-down, R_d, are defined as the maximum and minimum water-surface elevation measured vertically from the still-water level, SWL; as illustrated in Figure A.1.

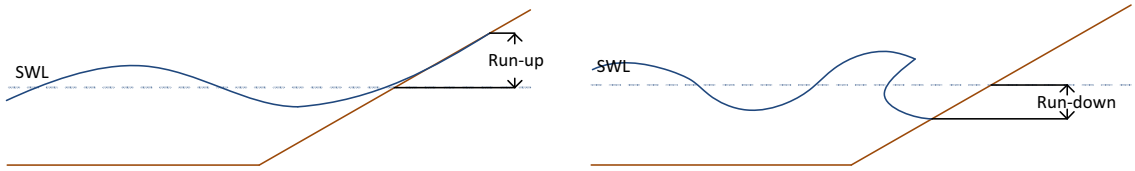

Figure A.1. **Left:** Run-up. **Right:** Run-down.

The run-up and run-down depend on:

d	water depth	$[m]$
H	wave height	$[m]$
T	wave period	$[s]$
β	wave attack angle	$[^\circ]$
α	slope angle	$[^\circ]$

In addition to the previously illustrated parameters, the surface roughness, the permeability, the porosity of the slope and type of wave breaking must also be taken into account when studying run-up and run-down effects.
The influence the run-up and run-down have over the armor layer greatly depends on both the magnitude and direction of the flow velocity vectors. The flow velocity vectors on a permeable surface for both run-up and run-down are illustrated below, in Figure A.2.

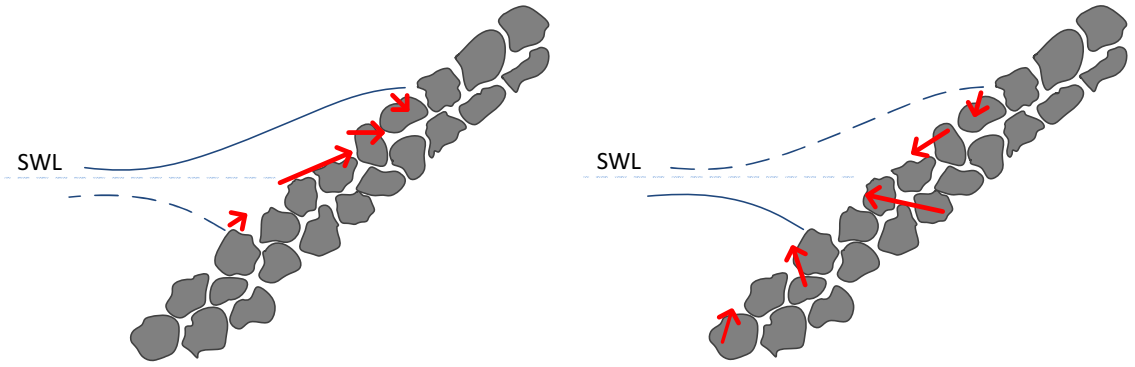

Figure A.2. Flow velocity vectors for run-up (**left**) and run-down (**right**)

It can be concluded that the largest destabilizing forces will occur during run-down and, in general, in a zone slightly below the SWL.

The forces acting on a single armor unit are illustrated in Figure A.3. Where F_D is the drag force, F_L is the lift force, F_G is the gravity force and F_R are the reaction forces in contact points between armor units. In this case, the flow is assumed to be quasi-stationary meaning that the inertia forces are neglected.

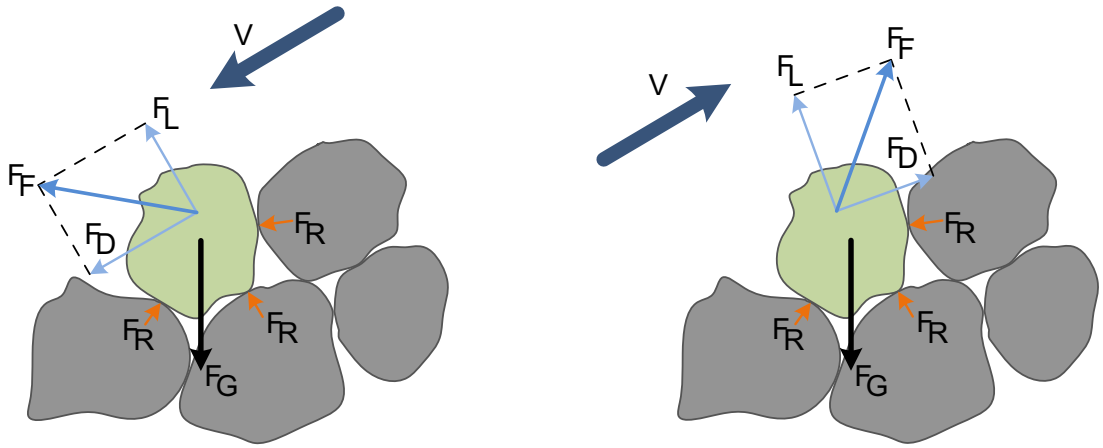

Figure A.3. Forces during run-down (**left**) and during run-up (**right**)

The lift force, F_L is caused by the difference in pressure between the upper and lower sides of the armor unit, due to the velocity difference.
The drag force, F_D depends on material roughness and geometry, in other words, skin friction and form drag force.
The gravity force, F_G is calculated as the weight of the armor unit from which the buoyancy is substrated.

As previously mentioned, the wave run-up and run-down depend also on the type of wave breaking. The breaker types can be identified by using the surf-similarity parameter, ξ, which can be found as follows:

$$\xi_o = \frac{tan(\alpha)}{\sqrt{s_0}} \text{ for regular waves} \tag{A.1}$$

$$\xi_{om} = \frac{tan(\alpha)}{\sqrt{s_{om}}} \text{ for irregular waves} \tag{A.2}$$

Where

α	slope angle		$[^\circ]$
s_0	deepwater wave steepness	$= H_0/L_0$	$[-]$
H_0	deepwater wave height		$[m]$
L_0	deepwater wave length	$= gT^2/2\pi$	$[m]$
T	wave period		$[s]$
g	gravitational acceleration		$[m/s^2]$
s_{om}	fictitious wave steepness	$= 2\pi H_s/gT_m^2$	$[-]$
H_s	significant wave height		$[m]$
T_m	mean wave period		$[s]$

The types of wave breaking can be cathegorised according to the surf-similarity parameter, as illustrated in Figure A.4 and Table A.1.

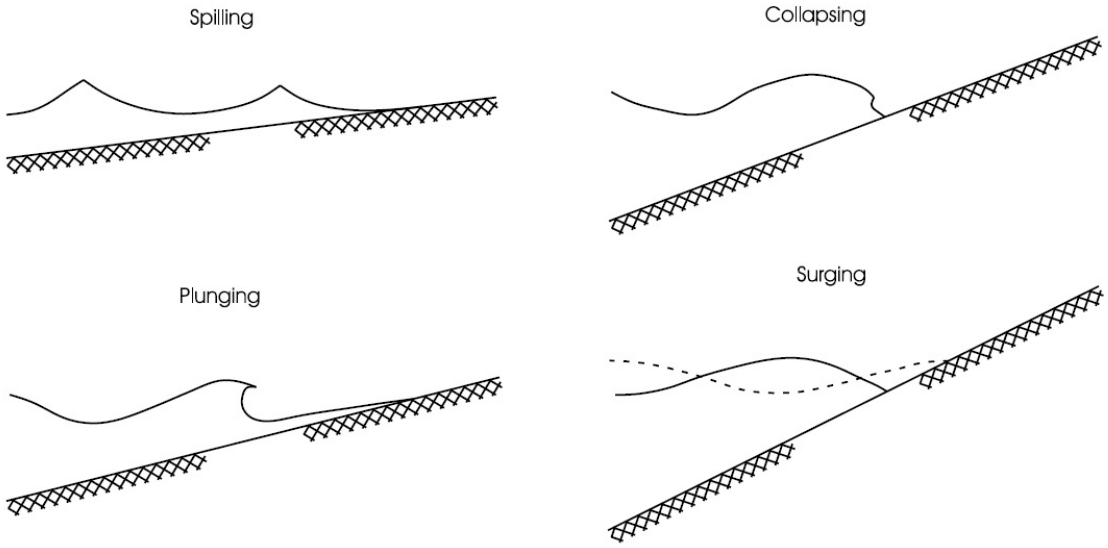

Figure A.4. Types of wave breaking, for regular waves. [T. Lykke Andersen et al. (2012)]

Table A.1. Wave breaking depeding on surf-similarity parameter.

Wave type	Surf-similarity parameter
Spilling	$\xi_o < 0.5$
Plunging	$0.5 < \xi_o < 3.3$
Collapsing	$\xi_o > 3.3$
Surging	$\xi_o > 3.3$

B Recession estimation

B.1 Lykke Andersen

The Lykke Andersen formula is given in Equation (B.1). In this section of the Appendix, a detiled description of the parameters of the equation is given.

$$\frac{Rec}{D_{n,50}} = f_{hb} \cdot \left[f_{H_0} \cdot \frac{2.2 \cdot h - 1.2 \cdot h_s}{h - h_b} \cdot f_\beta \cdot f_N \cdot f_{grad} \cdot f_{sk} - \frac{|cot(\alpha_d) - 1.05|}{2 \cdot D_{n,50}} \cdot (h - h_b) \right] \tag{B.1}$$

This formula was developed by evaluating the influence of different parameters, accounted for by factors presented and discussed here in Equations (B.2) to (B.7). Subsequenly, the parameters used in the equations are detailed in Equations (B.8) to (B.16). In the Lykke Andersen formula, and in Equations (B.2) to (B.16), the following symbols are used:

f_{hb}	berm elevation factor	$[-]$
f_{H_0}	stability index factor	$[-]$
f_β	incident wave angle factor	$[-]$
f_N	number of waves factor	$[-]$
f_{grad}	stone gradation factor	$[-]$
f_{sk}	skewness factor	$[-]$
h	water depth at toe	$[m]$
h_s	step height	$[m]$
h_b	water depth above berm	$[m]$
α_d	angle of the front slope	$[^\circ]$
β	incident wave angle of attack	$[^{circ}]$
H_{m0}	wave height	$[m]$
s_{0m}	steepness	$[-]$
g	gravitational acceleration	$[m/s^2]$
$T_{0,1}$	wave period	$[s]$
L_p	wave length	$[m]$
Ur	Ursell number	$[-]$
k_p	wave number	$[-]$

Berm elevation. It was discovered that the recession is much lower if the berm is below still water level. This reductoin in recession is takein into account by a reduction factor, f_{hb}.

$$f_{hb} = \begin{cases} 1 & for\ \frac{h_b}{H_{m0}} \leq 0.1 \\ 1.18 \cdot exp\left(-1.64 \cdot \frac{h_b}{H_{m0}}\right) & for\ \frac{h_b}{H_{m0}} > 0.1 \end{cases} \tag{B.2}$$

Incident wave angle. For head-on waves, β is taken as 0. Naturally, if the angle is increased, the parameters are reduced. This reduction is given by the factor f_β, as given

by van der Meer [1988].

$$f_\beta = cos(\beta) \tag{B.3}$$

Number of waves. The influence of the number of waves, as described by Lykke Andersen is commented in Section 2.4 of the present report.

$$f_N = \begin{cases} \left(\frac{N}{3000}\right)^{-0.046H_0+0.3} & for\ H_0 < 5 \\ \left(\frac{N}{3000}\right)^{0.07} & for\ H_0 > 5 \end{cases} \tag{B.4}$$

Stability indeces. The author of the article comments on the findings of van der Meer [1988] and Kao and Hall [1990]. A good fit for the data is obtained by introducing f_{H_0}, as shown in Equation (B.5). This parameter is proportional to $s_{0m}^{-0.05}$ in some cases, while in others the stability parameter H_0T_0 is used in the formula.

$$f_{H_0} = \begin{cases} 19.8 \cdot \left(\frac{-7.08}{H_0}\right) \cdot s_{0m}^{-0.5} & for\ T_0 \geq T_0^* \\ 0.05 \cdot H_0 T_0 + 10.5 & for\ T_0 < T_0^* \end{cases} \tag{B.5}$$

Skewness factor. Based on Lykke Andersen [2006], a parameter accounting for skewness is included, f_{sk}. The estimation of this factor is based on the Ursell number, given here in Equation (B.15).

$$f_{sk} = exp(1.5 \cdot b_1^2) \tag{B.6}$$

Grading factor. The article cites several earlier studies to assess stone gradation influence, such as Hall [1991] and van der Meer [1988]. Equation (B.7) gives the influence of the stone gradation.

$$f_{grad} = \begin{cases} 1 & for\ f_g \leq 1.5 \\ 0.43 \cdot f_g + 0.355 & for\ 1.5 < f_g < 2.5 \\ 1.43 & for\ f_g \geq 2.5 \end{cases} \tag{B.7}$$

$$f_g = \frac{D_{n,85}}{D_{n,15}} \tag{B.8}$$

Step height. On a reshaped profile, the step height is defined by Lykke Andersen and Burcharth [2009], as the point where the slope gets flatter than 1:2. The concept is illustrated in B.1. (!CONSIDER MOVING TO MAIN REPORT, to ilustrate the limits of hs>h)

$$h_s = 0.65 \cdot H_{m0} \cdot s_{0m}^{-0.3} \cdot f_N \cdot f_\beta \tag{B.9}$$

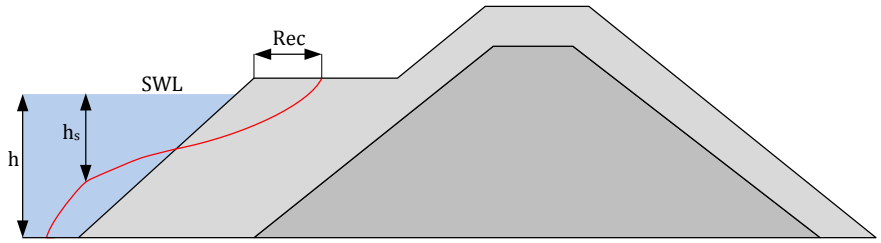

Figure B.1. Step height.

Further, other parameters used in this section are detailed.

$$H_0 = \frac{H_m 0}{\delta \cdot D_{n,50}} \tag{B.10}$$

$$T_0 = \sqrt{\frac{g}{D_{n,50}}} \cdot T_{0,1} \tag{B.11}$$

$$T_0^* = \frac{19.8 \cdot exp\left(\frac{-7.08}{H-0}\right) \cdot s_{0m}^{-0.5} - 10.5}{0.05 \cdot H_0} \tag{B.12}$$

$$s_{0m} = \frac{H_{m0}}{\frac{g}{2 \cdot \pi} \cdot T_{0,1}^2} \tag{B.13}$$

$$b_1 = 0.54 \cdot Ur^{0.54} \tag{B.14}$$

$$Ur = \frac{H_{m0}}{2 \cdot h \cdot (k_p \cdot h)^2} \tag{B.15}$$

$$k_p = \frac{2 \cdot \pi}{L_p} \tag{B.16}$$

B.2 Van der Meer

In this section it will be discussd in detail the relationships between different variables and and the parameters that define a profile, from van der Meer [1992] Figure B.2 shows the reshaped profile generated by applying the equations obtained by van der Meer, and detailed in this section.

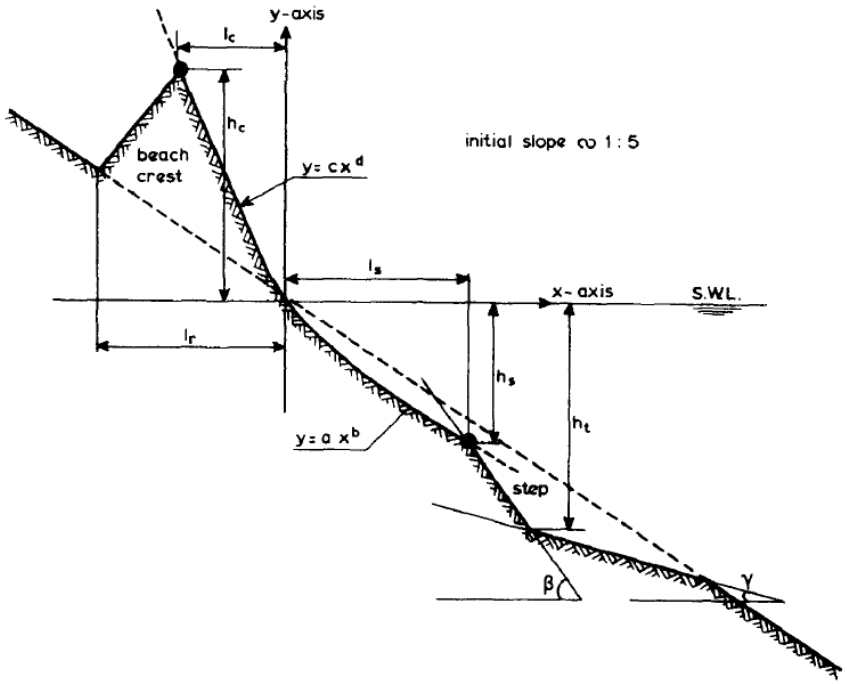

Figure B.2. Van der Meer's shematized profile [van der Meer, 1992].

van der Meer [1992] gives two equations for each profile parameter: one for the case of high H_0T_0, and one for low H_0T_0. Considering the purpose of this report, only the lower range of the H_0T_0 parameter is investigated. Equations (B.17) to (B.29) are the formulas selected for the present report.

Fictitious steepness, s_m

$$s_m = \frac{2 \cdot \pi \cdot H_s}{g \cdot T_m^2} \tag{B.17}$$

Stability parameter, H_0T_0

$$H_0T_0 = \frac{H_s}{\Delta \cdot D_{n,50}} \cdot \sqrt{\frac{g}{D_{n,50}}} \cdot T_m \tag{B.18}$$

Runup length, l_r

$$H_0T_0 = (20 - 1.5 \cdot cot\alpha) \cdot l_r / D_{n,50} \cdot N^{0.05} - 40 \tag{B.19}$$

Crest height, h_c

$$H_0T_0 = 33 \cdot \left(\frac{h_c}{D_{n,50} \cdot N^{0.15}} \right)^1 .3 + 30 \cdot cot\alpha - 30 \tag{B.20}$$

Crest length, l_c

$$H_0T_0 = (3 \cdot cot\alpha + 25) \cdot \frac{l_c}{D_{n,50} \cdot N^0.12} \tag{B.21}$$

Step height, h_s

$$H_0T_0 = 27 \cdot \left(\frac{h_s}{D_{n,50} \cdot N^{0.07}} \right)^1 .3 + 125 \cdot cot\alpha - 475 \tag{B.22}$$

Step length, l_s

$$H_0T_0 = 2.6 \cdot \left(\frac{l_s}{D_{n,50} \cdot N^{0.07}} \right)^1 .3 + 70 \cdot cot\alpha - 210 \tag{B.23}$$

The transition height, h_t

$$H_0T_0 = 10 \cdot \left(\frac{h_t}{D_{n,50} \cdot N^{0.04}} \right)^1 .3 + 175 cot\alpha - 725 \tag{B.24}$$

The profile is divided in two parts. The profile above SWL is described by Equation (B.25), and the profile below SWL is described by Equation (B.26). Coefficients a_1 and a_2, found in these equations, are determined by the values of the parameters obtained from Equations (B.17) to (B.24).

$$y = a_2 \cdot (-x)^{1.15} \tag{B.25}$$

$$y = a_1 \cdot x^{0.83} \tag{B.26}$$

The angle β

$$tan\beta = 1.1 tan\alpha^A \tag{B.27}$$

$$A = 1 - 0.45 \cdot exp\left(\frac{-500}{N} \right) \tag{B.28}$$

The angle γ

$$tan\gamma = 0.5 tan\alpha \tag{B.29}$$

B.2.1 *MatLab* program

A computer program is created using the equations from this chapter. In order to apply them, first some expressions need to be isolated for the profile parameters. This is done using Maple 16. After the expressions are isolated, they are implemented into *MatLab*.

$$h_c = \left(1/33\, H0T0 - \frac{10}{11}\, cotd\,(\alpha) + \frac{10}{11}\right)^{0.76} D_{n50} N^{0.15} \tag{B.30}$$

$$l_c = \frac{H0T0\, D_{n50} N^{0.12}}{3\, cotd\,(\alpha) + 25} \tag{B.31}$$

$$h_s = \left(1/27\, H0T0 - \frac{125}{27}\, cotd\,(\alpha) + \frac{475}{27}\right)^{0.76} D_{n50} N^{0.07} \tag{B.32}$$

$$l_s = 1.024 \times 10^{-97} \left((-0.97 - 0.23\, i)\left(4.69 \times 10^{125}\, H0T0 - 3.28 \times 10^{127}\, cotd\,(\alpha) + 9.85 \times 10^{127}\right)^{3/13}\right)^{10/3} D_{n50} N^{\frac{7}{100}} \tag{B.33}$$

$$h_t = \left(1/10\, H0T0 - \frac{35}{2}\, cotd\,(\alpha) + \frac{145}{2}\right)^{0.76} Dn50\, N^{0.04} \tag{B.34}$$

$$l_r = -\frac{(-H0T0 - 40)\, Dn50\, N^{0.05}}{20 - 1.5\, cotd\,(\alpha)} \tag{B.35}$$

Note that, to obtain the predicted recession in this case, only the top part of the generated profile i plotted over the initial profile of the model test. After plotting, the volume conservation is not accounted for and a measurement is taken for berm recession.

C Model testing

C.1 Test programme for the first configuration

Table C.1 shows the test programme for the configuration with a front slope of 1 : 1.1 and berm elevation of $0.04m$. The model is rebuilt after each test. This situation is named *low-berm, steep-slope* in the main report.

Table C.1. Program for model testing, 1xx.

Test Name	s_p [-]	H_s[m]	H_0[-]	T_p[s]	H_0T_0[-]
111	0.015	0.064	0.8	1.65	21
112		0.097	1.3	2.04	42.2
113		0.131	1.7	2.36	63.8
114		0.164	2.1	2.65	88.5
121	0.02	0.064	0.8	1.43	18.2
122		0.097	1.3	1.77	36.6
123		0.131	1.7	2.05	55.4
124		0.164	2.1	2.29	76.5
131	0.03	0.064	0.8	1.17	14.9
132		0.097	1.3	1.44	29.8
133		0.131	1.7	1.67	45.1
134		0.164	2.1	1.87	62.4
141	0.05	0.064	0.8	0.91	11.6
142		0.097	1.3	1.12	23.2
143		0.131	1.7	1.29	34.9
144		0.164	2.1	1.45	48.4
151	0.01	0.064	0.8	2.02	11.6
152		0.097	1.3	2.49	23.2
153		0.131	1.7	2.90	34.9

C.2 Test programme for the second configuration

Table C.2 shows the test programme for the configuration with a front slope of 1 : 1.5 and berm elevation of $0.04m$. The model is rebuilt after each test. This situation is named *low-berm, flat-slope* in the main report.

Table C.2. Program for model testing, 2xx.

Test Name	s_p [-]	H_s[m]	H_0[-]	T_p[s]	H_0T_0[-]
211	0.015	0.064	0.8	1.65	21
212		0.097	1.3	2.04	42.2
213		0.131	1.7	2.36	63.8
214		0.164	2.1	2.65	88.5
221	0.02	0.064	0.8	1.43	18.2
222		0.097	1.3	1.77	36.6
223		0.131	1.7	2.05	55.4
224		0.164	2.1	2.29	76.5
231	0.03	0.064	0.8	1.17	14.9
232		0.097	1.3	1.44	29.8
233		0.131	1.7	1.67	45.1
234		0.164	2.1	1.87	62.4
241	0.05	0.064	0.8	0.91	11.6
242		0.097	1.3	1.12	23.2
243		0.131	1.7	1.29	34.9
244		0.164	2.1	1.45	48.4
251	0.01	0.064	0.8	2.02	11.6
252		0.097	1.3	2.49	23.2
253		0.131	1.7	2.90	34.9

C.3 Test programme for the third configuration, progressing erosion

The tests for progressing erosion are done on a berm breakwater with a front slope of $1 : 1.25$ and berm elevation of $h_{br} = 0.04m$. A scan is taken after each series of waves. The model is not rebuilt between tests. The test programme for this configuration is shown in Table C.3.

Table C.3. Program for model testing, 3xx.

Test Name	s_p [-]	H_s[m]	H_0[-]	T_p[s]	Number of waves
300	0.045	0.164	2.1	1.53	250
301	0.045	0.164	2.1	1.53	250
302	0.045	0.164	2.1	1.53	250
303	0.045	0.164	2.1	1.53	250
304	0.045	0.164	2.1	1.53	250

C.4 Test programme for the fourth configuration, straight slope

Table C.4 shows the test programme for the 4^{th} configuration. This test series consists of 6 tests with a breakwater with no berm, and a straight front slope of 1:1.5. The model is rebuilt after each test. This situation is named *straight slope* in the main report.

Table C.4. Program for model testing, 5xx.

Test Name	s_p [-]	H_s[m]	H_0[-]	T_p[s]	H_0T_0[-]
511	0.015	0.064	0.8	1.65	21
512		0.097	1.3	2.04	42.2
513		0.131	1.7	2.36	63.8
514		0.164	2.1	2.65	88.5
522	0.02	0.097	1.3	1.77	36.6
523		0.131	1.7	2.05	55.4

C.5 Test programme for the fifth configuration

Table C.5 shows the test programme for the configuration with a front slope of 1 : 1.1 and berm elevation of $0.07m$. The model is rebuilt after each test. This situation is named *high-berm, steep-slope* in the main report.

Table C.5. Program for model testing, 6xx.

Test Name	s_p [-]	H_s[m]	H_0[-]	T_p[s]	H_0T_0[-]
612	0.015	0.097	1.3	2.04	42.2
613		0.131	1.7	2.36	63.8
622	0.02	0.097	1.3	1.77	36.6
623		0.131	1.7	2.05	55.4
652	0.01	0.097	1.3	2.49	23.2
653		0.131	1.7	2.90	34.9

D Results and discussion

Figure D.1 shows the comparison between all the recession estimation methods evaluated in this report. Note that the formulas are plotted with the adjusted parameters, as concluded by this report. Table D.1 contains a symbols convention used in the analysis part of this paper, and serves as a legend for Figure D.1.

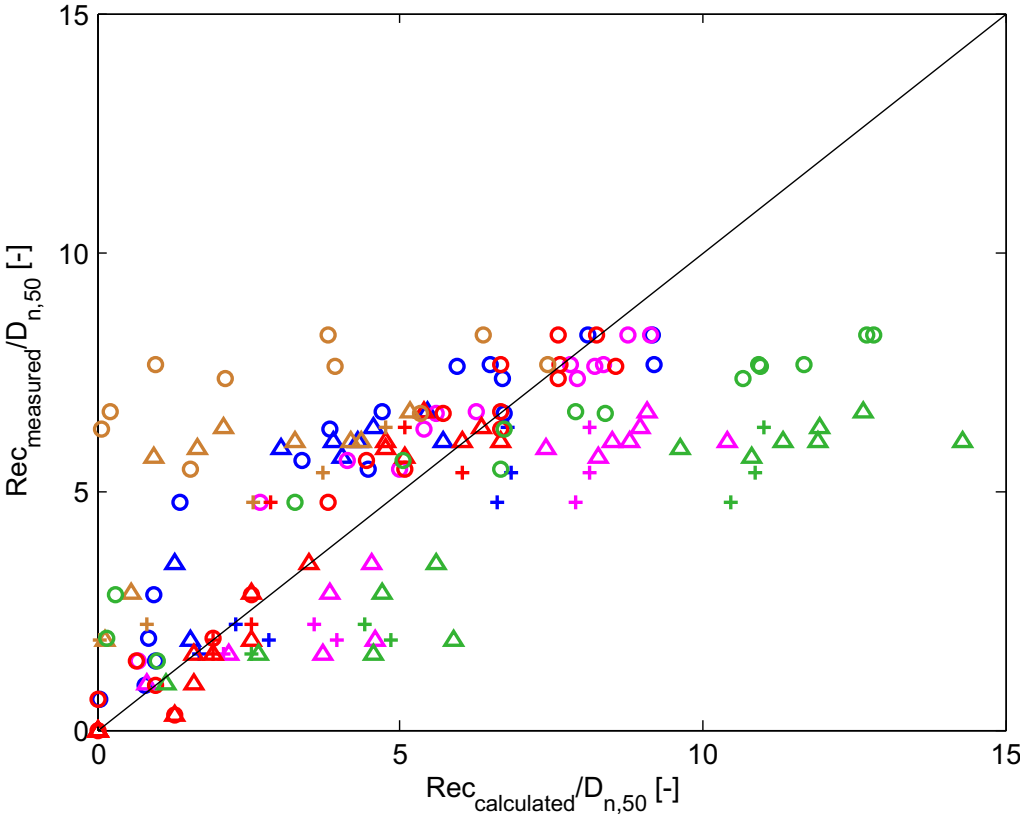

Figure D.1. Comparison of all methods.

Table D.1. Symbol convention, legend for D.1.

Berm elevation:	$0.04[m]$	$0.04[m]$	$0.07[m]$
Front slope:	1:1.1	1:1.5	1:1.1
Lykke-Andersen	○	△	+
Moghim	○	△	+
van der Meer	○	△	+
Tørum	○	△	+
Shekari	○	△	+

E Electronic appendix

A large number of electronic data files have been generated during the course of laboratory experiments and data analysis. This appendix contains lists of the data files and computer programs that are available on the DVD enclosed with this report. In the fpllowing sections, a short description will be given about the contents of the respective ennumerated files.

E.1 *EPro* data files

These files can be open using *EPro* and contains the project file used by the researchers of this project. It contains all the scanned profiles that have also been saved as *Excel* files. A list of those files will be provided in this appendix.

1. i1.EEP
2. i1.tee
3. i1.txt

E.2 *MatLab* files

These files can be open using *MatLab*. The list contains both *.m* and *.mat* files, scripts, functions and saved variables.

1. com_MOG
2. com_TLA
3. com_vdm
4. Conversion
5. dimrec_orig
6. dimrec_mod
7. dimrec_zero
8. MAIN_comparison
9. MAIN_erosion
10. Main_VDM
11. rec_MOG
12. Rec_SH
13. rec_tla_tor

E.3 *WaveLab* data files

The files listed below can be opened using *WaveLab*. They contained the data recorded by the six wave gauges during the tests. The names of the files correspond to test names.

1. 111.dat
2. 112.dat
3. 113.dat
4. 114.dat
5. 121.dat
6. 122.dat
7. 123.dat
8. 124.dat
9. 131.dat
10. 132.dat
11. 133.dat
12. 134.dat
13. 141.dat
14. 142.dat
15. 143.dat
16. 144.dat
17. 151.dat
18. 152.dat
19. 153.dat
20. 211.dat
21. 212.dat
22. 213.dat
23. 214.dat
24. 221.dat
25. 222.dat
26. 223.dat
27. 224.dat
28. 231.dat
29. 232.dat
30. 233.dat
31. 234.dat
32. 241.dat
33. 242.dat
34. 243.dat
35. 244.dat
36. 251.dat
37. 252.dat
38. 253.dat
39. 300.dat
40. 301.dat
41. 302.dat
42. 303.dat
43. 304.dat
44. 511.dat
45. 512.dat
46. 513.dat
47. 514.dat
48. 522.dat
49. 523.dat
50. 612.dat
51. 613.dat
52. 622.dat
53. 623.dat
54. 622.dat
55. 623.dat

E.4 *Excel* files

These *.xls* can be open using *Excel 2003* or newer versions. They contain test results from time-domain and frequency domain analysis in *WaveLab*, as well as the *EPro* generated files that contain the scanned profiles.

E.4.1 Results files

1. Test_program-Final

E.4.2 Profiling data

The following list contains the excel files generated by *EPro*, containing initial and final profile scans.

1. initial_111
2. final_111
3. initial_112
4. final_112
5. initial_113
6. final_113
7. initial_114
8. final_114
9. initial_121
10. final_121
11. initial_122
12. final_122
13. initial_123
14. final_123
15. initial_124
16. final_124
17. initial_131
18. final_131
19. initial_132
20. final_132
21. initial_133
22. final_133
23. initial_134
24. final_134
25. initial_141
26. final_141
27. initial_142
28. final_142
29. initial_143
30. final_143
31. initial_144
32. final_144
33. initial_151
34. final_151
35. initial_152
36. final_152
37. initial_153
38. final_153
39. initial_211
40. final_211
41. initial_212
42. final_212
43. initial_213
44. final_213
45. initial_214
46. final_214
47. initial_221
48. final_221
49. initial_222
50. final_222
51. initial_223
52. final_223
53. initial_224
54. final_224
55. initial_231
56. final_231
57. initial_232
58. final_232
59. initial_233
60. final_233
61. initial_234
62. final_234
63. initial_241
64. final_241
65. initial_242
66. final_242
67. initial_243
68. final_243
69. initial_244
70. final_244
71. initial_251
72. final_251
73. initial_252
74. final_252
75. initial_253

76. final_253
77. initial_300
78. final_300
79. initial_301
80. final_301
81. initial_302
82. final_302
83. initial_303
84. final_303
85. initial_304
86. final_304
87. initial_511
88. final_511
89. initial_512
90. final_512
91. initial_513
92. final_513
93. initial_514
94. final_514
95. initial_522
96. final_522
97. initial_523
98. final_523
99. initial_612
100. final_612
101. initial_613
102. final_613
103. initial_622
104. final_622
105. initial_623
106. final_623
107. initial_652
108. final_652
109. initial_653
110. final_653